Targeting L-type amino acid transporter 1 in innate and adaptive T cells efficiently controls skin inflammation

Danay Cibrian, PhD,[a,b,c]* Raquel Castillo-González, MS,[a,b]* Nieves Fernández-Gallego, MS,[a,b] Hortensia de la Fuente, MD, PhD,[a,b,c] Inmaculada Jorge, PhD,[b,c] María Laura Saiz, PhD,[a,b] Carmen Punzón, MTA,[d] Marta Ramírez-Huesca, MTA,[b] Miguel Vicente-Manzanares, PhD,[e] Manuel Fresno, PhD,[d] Esteban Daudén, MD, PhD,[f] Javier Fraga-Fernandez, MD, PhD,[f] Jesús Vazquez, PhD,[b,c] Julián Aragonés, PhD,[c,g] and Francisco Sánchez-Madrid, PhD[a,b,c]* *Madrid and Salamanca, Spain*

GRAPHICAL ABSTRACT

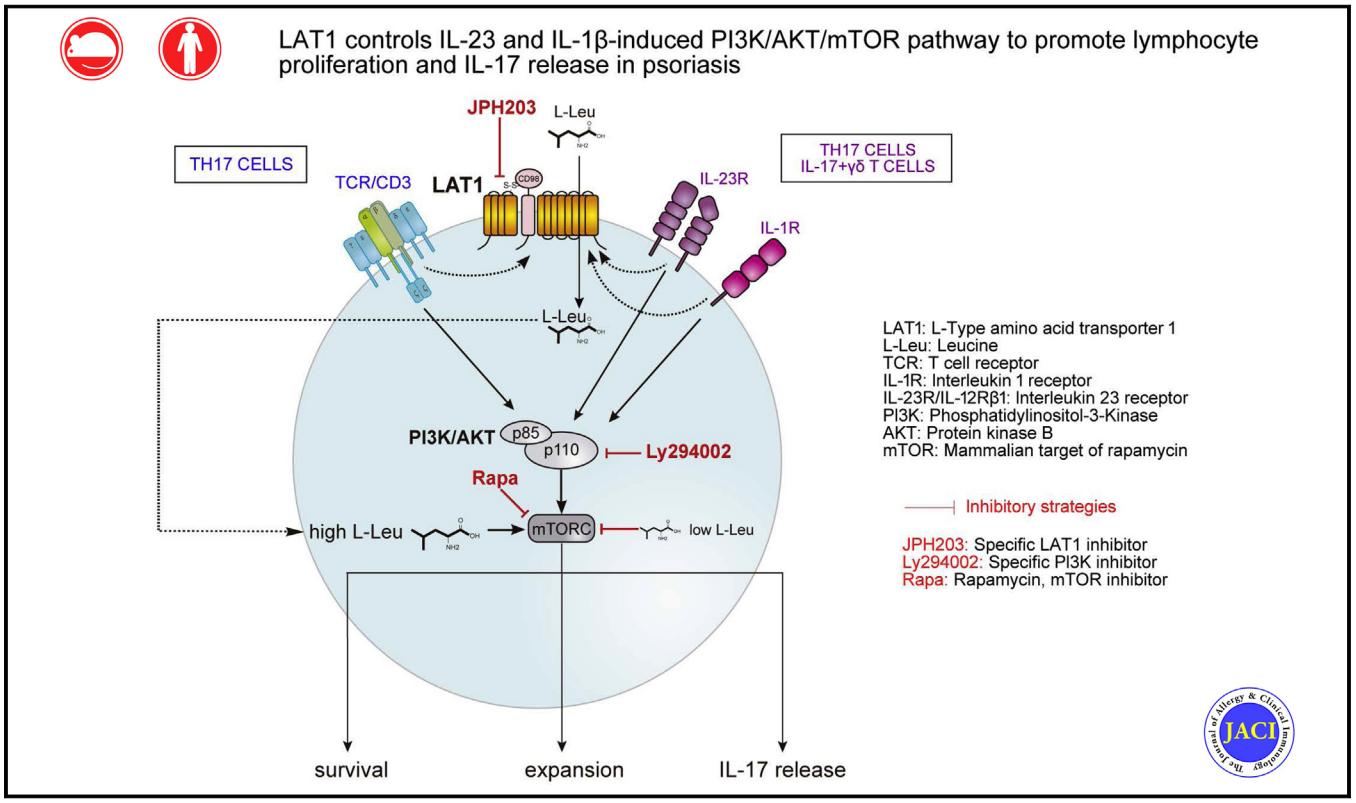

From [a]the Immunology Service, Hospital de la Princesa, Instituto Investigación Sanitaria Princesa, Universidad Autónoma de Madrid (UAM), Madrid; [b]Centro Nacional de Investigaciones Cardiovasculares (CNIC), Madrid; [c]CIBER de Enfermedades Cardiovasculares, Carlos III Health Institute, Madrid; [d]Centro de Biología Molecular Severo Ochoa (CSIC-UAM), Madrid; [e]Centro de Investigación del Cáncer-Instituto de Biología Molecular y Celular del Cáncer, CIC-IBMCC (CSIC-Universidad de Salamanca), Salamanca; [f]the Dermatology Service, Hospital de la Princesa, Madrid; and [g]the Reasearch Unit, Hospital de La Princesa, Instituto Investigación Sanitaria Princesa, Universidad Autónoma de Madrid.

*These authors contributed equally to this work.

Supported by grants SAF 2017-82886-R (to F.S.-M.), PI17/01972 (to E.D.), and SAF 2013-42850-R (to M.F.) from the Spanish Ministry of Economy and Competitiveness; CAM (S2017/BMD-3671-INFLAMUNE-CM) from the Comunidad de Madrid (to F.S.-M.); and CIBERCV, BIOIMID PIE13/041 from Instituto de Salud Carlos III and Fundación La Marató TV3 (20152330 31). The project leading to these results has also received funding from FUNDACIÓN BBVA A EQUIPOS DE INVESTIGACIÓN CIENTÍFICA 2018 and from "la Caixa" Banking Foundation under the project code HR17-00016 (to F.S.-M.) and from Agencia Estatal de Investigación, Fondo Europeo de Desarrollo Regional, European Union.

Disclosure of potential conflict of interest: The authors declare that they have no relevant conflicts of interest.

Received for publication April 4, 2019; revised September 9, 2019; accepted for publication September 16, 2019.

Available online October 9, 2019.

Corresponding author: Francisco Sánchez-Madrid, PhD, Instituto Investigación Sanitaria Princesa IIS-IP, Diego de León 62, 28006 Madrid, Spain. E-mail: fsmadrid@salud.madrid.org.

The CrossMark symbol notifies online readers when updates have been made to the article such as errata or minor corrections

0091-6749

https://doi.org/10.1016/j.jaci.2019.09.025

Background: Psoriasis is a frequent inflammatory skin disease that is mainly mediated by IL-23, IL-1β, and IL-17 cytokines. Although psoriasis is a hyperproliferative skin disorder, the possible role of amino acid transporters has remained unexplored.

Objective: We sought to investigate the role of the essential amino acid transporter L-type amino acid transporter (LAT) 1 (SLC7A5) in psoriasis.

Methods: LAT1 floxed mice were crossed to Cre-expressing mouse strains under the control of keratin 5, CD4, and retinoic acid receptor–related orphan receptor γ. We produced models of skin inflammation induced by imiquimod (IMQ) and IL-23 and tested the effect of inhibiting LAT1 (JPH203) and mammalian target of rapamycin (mTOR [rapamycin]).

Results: LAT1 expression is increased in keratinocytes and skin-infiltrating lymphocytes of psoriatic lesions in human subjects and mice. LAT1 deletion in keratinocytes does not dampen the inflammatory response or their proliferation, which could be maintained by increased expression of the alternative amino acid transporters LAT2 and LAT3. Specific deletion of LAT1 in γδ and CD4 T cells controls the inflammatory response induced by IMQ. LAT1 deletion or inhibition blocks expansion of IL-17–secreting $\gamma4^+\delta4^+$ and CD4 T cells and dampens the release of IL-1β, IL-17, and IL-22 in the IMQ-induced model. Moreover, inhibition of LAT1 blocks expansion of human γδ T cells and IL-17 secretion by human CD4 T cells. IL-23 and IL-1β stimulation upregulates LAT1 expression and induces mTOR activation in IL-17$^+$ γδ and T_H17 cells. Deletion or inhibition of LAT1 efficiently controls IL-23– and IL-1β–induced phosphatidylinositol 3-kinase/AKT/mTOR activation independent of T-cell receptor signaling.

Conclusion: Targeting LAT1-mediated amino acid uptake is a potentially useful immunosuppressive strategy to control skin inflammation mediated by the IL-23/IL-1β/IL-17 axis. (J Allergy Clin Immunol 2020;145:199-214.)

Key words: *L-type amino acid transporter 1, SLC7A5, psoriasis, γδ T cells, T_H17, mammalian target of rapamycin*

Abbreviations used

AHR:	Aryl hydrocarbon receptor
BrdU:	Bromodeoxyuridine
DMSO:	Dimethyl sulfoxide
FC:	Flow cytometry
H&E:	Hematoxylin and eosin
IL-1R:	IL-1 receptor
IMQ:	Imiquimod
K5:	Keratin 5
LAT:	L-type amino acid transporter
L-Leu:	L-leucine
mTOR:	Mammalian target of rapamycin
NF-κB:	Nuclear factor κ-light-chain-enhancer of activated B cells
PI3K:	Phosphatidylinositol 3-kinase
PMA:	Phorbol 12-myristate 13-acetate
P-S6:	Phospho-S6 ribosomal protein
RORγt:	Retinoic acid receptor–related orphan receptor γ
TCR:	T-cell receptor
WT:	Wild-type

Psoriasis is a common skin disorder characterized by formation of focal plaques of inflamed and raised skin with squamous appearance.[1] The affected portions of the skin show massive keratinocyte proliferation and prominent infiltration of immune cells, suggesting that psoriasis is a primary disorder of the skin immune system.[1-3] As in patients with other chronic inflammatory diseases, the proinflammatory cytokines IL-23, IL-1β, and IL-17 exert important functions in patients with psoriasis.[4-6]

Human psoriatic skin showed increased numbers of IL-17–releasing γδ and T_H17 cells,[7] as were also seen in murine models induced by topical application of the Toll-like receptor 7/8 agonist imiquimod (IMQ) or IL-23 injections.[8-10] Increased numbers of dermal macrophages, dendritic cells, and keratinocytes secreting IL-1β and IL-23 are also described.[8] IL-23 stimulates the survival and proliferation of T_H17 cells, whereas IL-1 receptor (IL-1R)–deficient mice do not properly display T_H17 cells.[11] However, the molecular mechanism by which IL-23 receptor and IL-1R contribute to the development, survival, and expansion of IL-17 cells remains unclear. Importantly, IL-1β potentiates the effects of IL-23 by inducing expression of IL-23 receptor in both T_H17 and γδ T cells.[11,12]

L-type amino acid transporter (LAT) 1 (SLC7A5) is a 512 amino acid–long, 12-transmembrane protein that mediates sodium-independent large neutral amino acid transport.[13] LAT1 (light chain) forms a heterodimeric complex with CD98/SLC3A2 (heavy chain) through disulfide bonds.[14] Heterodimerization stabilizes and enhances LAT1 transport to the plasma membrane, making it fully functional.[15] The alternative amino acid transporters LAT2/SLC7A8, LAT3/SLC43A1, and LAT4/SLC43A2 can also mediate large neutral amino acid uptake.[16] However, LAT1 is the main L-leucine (L-Leu) transporter expressed in T-cell receptor (TCR)–activated T cells[17] and natural killer cells.[18]

The expression of LAT1 is increased in many cancer cells,[19] including malignant skin lesions.[20] LAT1 is the main mediator of L-Leu uptake in malignant cells, and its usefulness as a target to inhibit cancer proliferation has been explored. Accordingly, the novel LAT1-specific inhibitor JPH203 has emerged as a promising cancer therapy that blocks the phosphatidylinositol 3-kinase (PI3K)/AKT/mammalian target of rapamycin (mTOR) pathway.[21]

Previously, we showed that CD69 regulates L-tryptophan uptake through LAT1, which contributes to aryl hydrocarbon receptor (AHR) activation in skin-resident γδ T cells.[22] In addition, LAT1 regulates L-Leu transport in CD4 T cells, controlling mTOR activation induced by TCR signaling.[17] However, a direct contribution of LAT1 to skin inflammation *in vivo* remains unexplored.

Here we use a conditional (floxed) LAT1 knockout mouse ($LAT1^{fl/fl}$)[17] to assess the role of LAT1 in keratinocyte proliferation and in CD4 and γδ T-cell function in an *in vivo* model of psoriasis induced by IMQ. Our results show that LAT1 deletion does not affect keratinocyte proliferation, whereas it effectively prevents expansion of IL-17–releasing immune cells. The data herein demonstrate that LAT1 inhibition shuts down the PI3K/AKT/mTOR axis induced by IL-23 and IL-1β in immune cells, becoming a promising novel strategy to control the inflammatory response that underlies the onset and course of psoriasis.

METHODS

A complete and detailed description of the methods used in this study are presented in the Methods section in this article's Online Repository at www.jacionline.org.

Mice

LAT1 floxed mice have been previously described.[17] CD4-Cre and retinoic acid receptor–related orphan receptor γ (RORγt)–Cre mice were purchased from the Jackson Laboratory (Bar Harbor, Me). Remaining mouse strains, such as Krt5-CreERT2 mice, were kindly provided by different groups.

Human subjects

Skin punch biopsy specimens (3 mm) and blood samples were obtained from patients with psoriasis and healthy volunteers. The study was approved by the Hospital Universitario de La Princesa ethics committee, and all participants provided written informed consent.

Psoriasis model

IMQ-induced[8,23] and an IL-23–induced[22] murine models of skin inflammation were used, as described previously.

Histologic analysis

Skin samples (from mice and human subjects) were processed for hematoxylin and eosin (H&E) staining and analysis of LAT1, LAT2, LAT3, and IL-17 expression by using immunohistochemical and immunofluorescence techniques.

Flow cytometry analysis and *in vitro* stimulation

Single-cell suspensions from mouse skin, blood, and lymph nodes were stained with a mixture of appropriate anti-mouse antibodies and analyzed by using flow cytometry (FC) technique. Total PBMCs or purified CD4 T cells from healthy donors and patients with psoriasis were also analyzed by using FC after staining with corresponding antibodies (see Table E1 in this article's Online Repository at www.jacionline.org). The sequence of used primers are listed in Table E2.

Human and mouse cell suspensions were *in vitro* stimulated with IL-23, IL-1β, or both (10 ng/mL each) to analyze cytokine release (IL-17, IL-22, and IFN-γ), proliferation (Ki-67 and bromodeoxyuridine [BrdU]), and phospho-S6 ribosomal protein (P-S6) expression.

Amino acid assessments

The serum L-Leu profile of normal (wild-type [WT]) and *Rag1*$^{-/-}$ mice treated or not with IMQ (for 5 days, 50 mg/d) were measured by using liquid chromatography–tandem mass spectrometry.

Uptake of the ^{3}H-radiolabeled amino acids L-phenylalanine and L-Leu (PerkinElmer, Waltham, Mass) was assessed in activated CD4 T cells from LAT1^{WT}, LAT1$^{\Delta R\gamma t}$, and LAT1$^{\Delta CD4}$ mice, according to the protocol described previously.[22]

Statistical analysis

Results were reported as mean ± SEMs. Statistical evaluations were performed with GraphPad Prism 7 software (GraphPad Software, La Jolla, Calif). Normality of data distribution was assessed by using the Kolmogorov-Smirnov test. The 2-tailed Student *t* test or Mann-Whitney test was used for comparison of 2 populations. Multiple comparisons were performed by using 1-way or 2-way ANOVA, followed by *post hoc* (Bonferroni) tests. A *P* value of less than .05 was considered significant.

RESULTS

Expression of the essential amino acid transporter LAT1 in psoriasis

To assess the relevance of essential amino acids in psoriasis, we evaluated levels of L-Leu in normal (WT) and immunodeficient (*Rag1*$^{-/-}$) mice treated or not with IMQ. Circulating levels of L-Leu in *Rag1*$^{-/-}$ mice were increased compared with those in WT mice, suggesting that essential amino acids are likely modulated by adaptive B or T cells in the IMQ model (Fig 1, *A*).

Normal skin is characterized by LAT2 expression, whereas LAT1 mainly appears in several different types of malignant skin lesions.[24,25] Our results clearly showed that LAT1 expression is induced in keratinocytes and lymphocytes in human psoriatic skin (Fig 1, *B* and *C*), as well as in mouse skin after IMQ application (Fig 1, *D*). Further analysis showed that dermal IL-17^{+} cells observed in mice treated with IMQ express LAT1 (Fig 1, *E*).

Considering the high expression of LAT1 in the epidermal layer of patients with psoriasis, we examined the effect of deleting LAT1 in keratinocytes. Mice carrying floxed LAT1 alleles (LAT1$^{fl/fl}$)[17] were crossed with mice expressing the Cre recombinase controlled by the keratinocyte-specific keratin 5 (K5) promoter (K5-CreERT2 mice)[26] and Rosa26-floxed stop tdTomato (Tm) mice.[27] This system fluorescently labels the cells that successfully underwent LAT1 deletion. After tamoxifen administration, mice displaying fluorescently red skin from both genotypes, LAT1^{WT} and LAT1$^{\Delta K5}$, were selected for topical treatment with IMQ. Both groups developed psoriasis after IMQ application independent of LAT1 expression in keratinocytes (Fig 2, *A*). The increase in epidermal thickness was similar in both genotypes (Fig 2, *B*). Neutrophil and macrophage infiltration also increased upon IMQ application independent of LAT1 expression in epidermal cells (Fig 2, *C*). Cre recombinase, as determined by Tm expression, was not detected in inflammatory cells (data not shown).

Analysis of Tm^{+} keratinocytes (CD49f^{+}) confirmed deletion of LAT1 expression after tamoxifen administration (Fig 2, *D*). The proliferation markers Ki-67 and BrdU revealed that deletion of LAT1 does not affect keratinocyte proliferation (Fig 2, *E*). These results indicate that essential amino acid uptake in these cells does not require LAT1 and could be mediated by other amino acid transporters, such as LAT2 or LAT3, which can also shuttle L-Leu.[16] LAT2 is broadly expressed in keratinocytes in normal human skin and increased in psoriatic lesions (see Fig E1, *A*, in this article's Online Repository at www.jacionline.org). Epithelial cells, such as HaCat and Caco-2 cells, express LAT2 and LAT1, whereas Hela and lymphoid cells only express LAT1 (see Fig E1, *B*). Moreover, LAT2 expression in keratinocytes increased in LAT1$^{\Delta K5}$ and LAT1^{WT} mice after IMQ application (see Fig E1, *C*). Finally, high expression of LAT3 was observed in the basal layer of keratinocytes of normal human skin and psoriatic lesions (see Fig E1, *D*). These data indicate that psoriasis increases the expression of several essential amino acid transporters in keratinocytes to support enhanced proliferation.

IL-17^{+} secreting cells detected in the skin of IMQ-treated mice are mainly Vγ4^{+}δ4^{+} and CD4 T cells.[28] Importantly, the proliferative response of Vγ4^{+}δ4^{+} (Fig 2, *F*) and CD4 (Fig 2, *G*) T cells induced in the draining lymph nodes after IMQ application was similar in both mouse groups independent of LAT1 expression in keratinocytes.

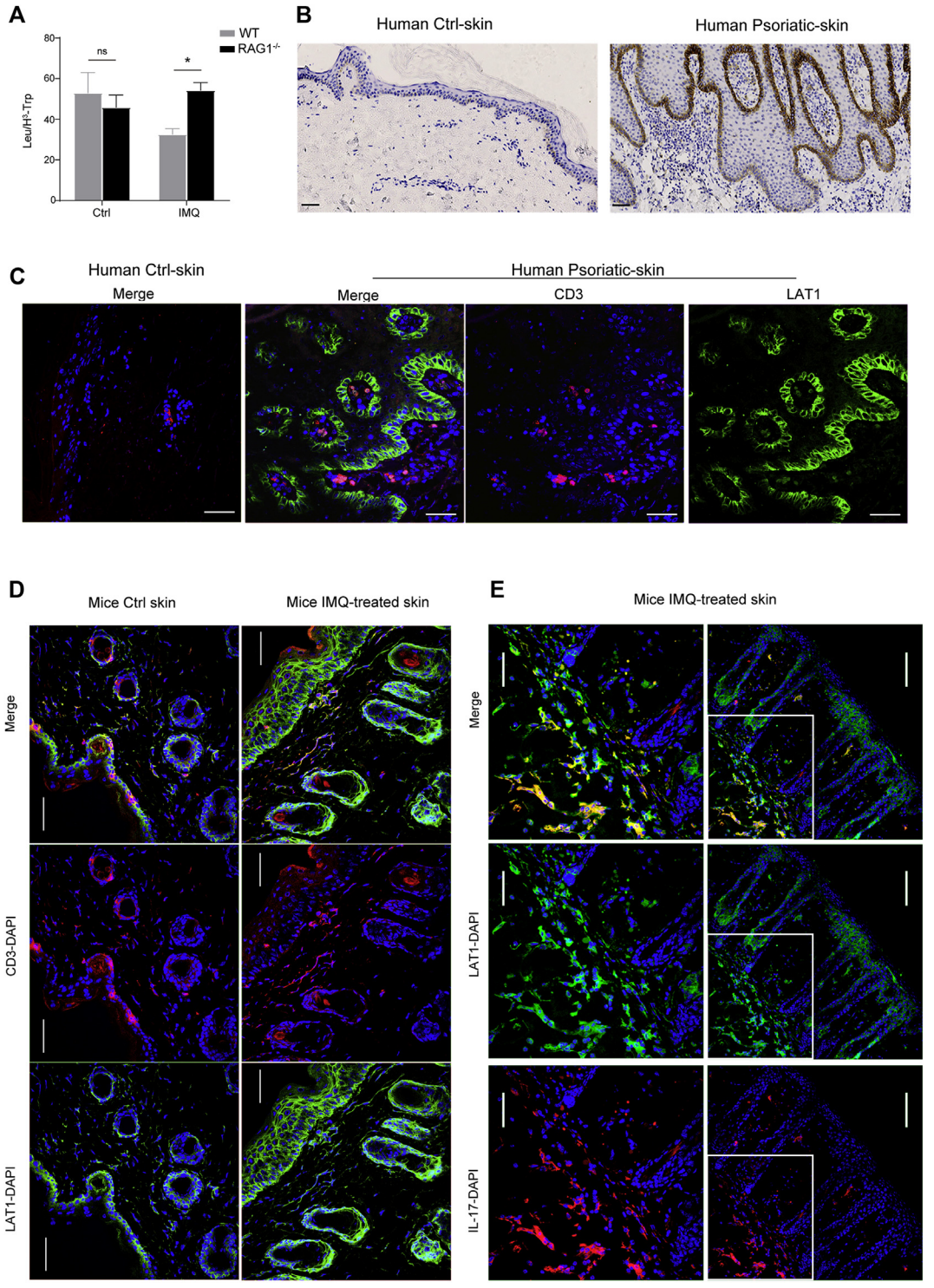

FIG 1. Expression of the amino acid transporter LAT1 is induced in patients with psoriasis and in the IMQ model. **A,** Relative levels of L-Leu detected by using mass spectrometry in sera of healthy *(Ctrl)* and IMQ-treated WT and *Rag1*$^{-/-}$ mice (n = 4-6 mice). *Bars* indicate means ± SEMs. *ns,* Not significant. **P* < .05, 2-tailed unpaired Student *t* test. **B,** LAT1 detection by means of immunohistochemistry in skin biopsy specimens from healthy donors and patients with psoriasis. **C,** Representative immunofluorescence of LAT1 (green) and CD3 (red) in skin samples from healthy donors and patients with psoriasis. **D,** Immunofluorescence of LAT1 (green) and CD3 (red) in dorsal skin of WT mice after IMQ and control skin. **E,** Detection of LAT1 (green) expression in dermal cells secreting IL-17 (red) in mice treated with IMQ for 4 days. Zoom areas *(left)* are indicated by the *white box (right)*. Nuclei were always stained with 4′-6-diamidino-2-phenylindole dihydrochloride (*DAPI*; blue). *Scale bars* = 100 and 50 μm in zoom area. At least 3 skin biopsy specimens of mouse or human origin were simultaneously analyzed in each experiment.

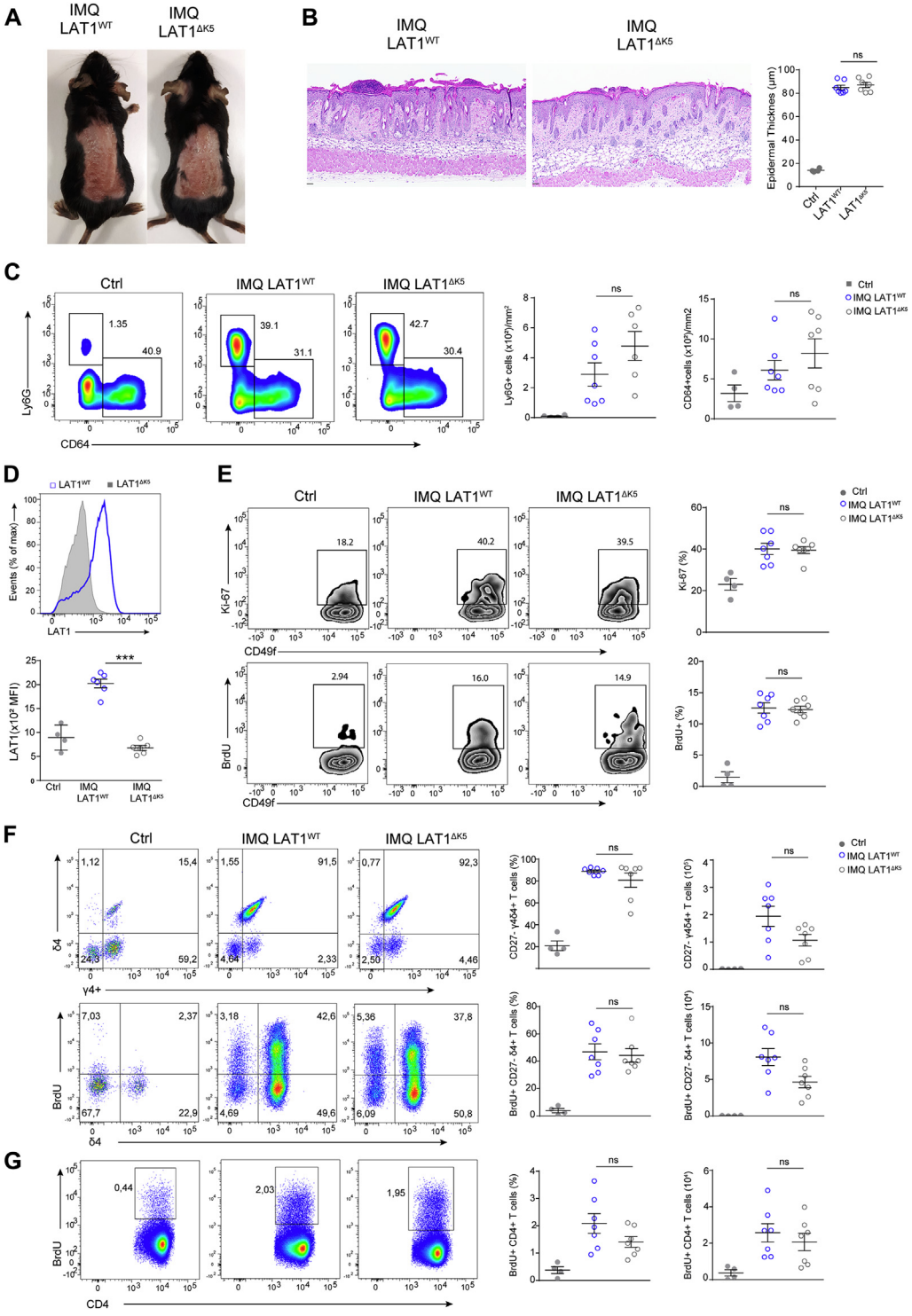

FIG 2. Deletion of LAT1 in keratinocytes does not affect psoriasis induced by IMQ. **A,** Representative pictures of LAT1^{WT} and LAT1$^{\Delta k5}$ mice after IMQ application. **B,** Representative H&E skin sections per group. *Scale bars* = 100 μm. Averaged values of epidermal thickness per mice are shown in the graphic at right. **C,** Representative density plots of skin neutrophil (Ly6G$^+$; *top*) and macrophage (CD64$^+$; *right*) populations on CD45$^+$ live cells. Density values of cells are shown in the graphics. **D,** Histogram *(upper)* and individual values *(bottom)* of LAT1 fluorescence in live keratinocytes. **E,** Density plots *(left)* and individual values of frequencies *(right)* of Ki-67$^+$ *(upper panels)* and BrdU$^+$ *(lower panels)* cells from live keratinocytes. **F,** Dot plots of Vγ4$^+$δ4$^+$ *(upper)* and BrdU$^+$δ4$^+$ *(bottom)* cells from live CD27$^-$ γδ T cells quantified in the lymph nodes. **G,** Dot plots of the frequency of BrdU$^+$ CD4 T cells in lymph nodes. Individual values of frequencies *(left)* and total cell numbers *(right)* are shown in the graphs (Fig 2, *F* and *G*). A representative experiment of 2 is shown (n = 4-7 per group). Data are represented as means ± SEMs. *ns,* Not significant. ***$P < .001$, 1-way ANOVA with the Bonferroni *post hoc* test (Fig 2, *B-G*).

LAT1 deletion in innate and adaptive T cells prevents psoriasis

To simultaneously study the function of LAT1 in adaptive and innate lymphocytes, we crossed $LAT1^{fl/fl}$ mice[17] with RORγt-$Cre^{+/-}$ mice[29] and Rosa26-floxed stop tdTomato mice.[27] Characterization of $LAT1^{\Delta R\gamma t}$ mice revealed that specific deletion of LAT1 in the skin occurs in cells that had expressed and/or were expressing RORγt, including dermal γδ T cells, skin-resident type 3 innate lymphoid cells, and skin CD4 T cells (see Fig E2, *A*, in this article's Online Repository at www.jacionline.org). Expression of Cre-recombinase was detected in $CD27^-$ γδ T cells within lymph nodes (see Fig E2, *B*). These are mainly IL-17–secreting cells that also express RORγt.[30] Moreover, because RORγt is also expressed during T-cell development at the immature double-positive stage in the thymus,[31] deletion of LAT1 can occur also in most TCRαβ T-cell subsets (see Fig E2, *B*). Indeed, *in vitro*–activated CD4 T cells from $LAT1^{\Delta R\gamma t}$ mice did not express LAT1 (see Fig E2, *C*). Also, these cells were smaller and less complex (see Fig E2, D) and displayed defective amino acid uptake (see Fig E2, E).

To ascertain whether deletion of LAT1 in $ROR\gamma t^+$ cells could affect skin lymphocyte populations at steady state, we analyzed the distribution of different skin $CD3^+$ T-cell subsets. No significant differences in the frequency or absolute numbers of dermal CD4 and γδ T cells, which were mostly Tm^+, were detected in $LAT1^{\Delta R\gamma t}$ and $LAT1^{WT}$ mice at steady state (see Fig E2, *F*). Epidermal γδ T cells (dendritic epidermal T cells), which were identified by greater TCR expression, did not express RORγt or Tm and were otherwise unaffected by LAT1 deletion in the other subsets (see Fig E2, *F*).

Compared with $LAT1^{WT}$ mice, induction of psoriasis in $LAT1^{\Delta R\gamma t}$ mice was clearly reduced, with a smaller area affected and an almost complete absence of redness and squamous appearance (Fig 3, *A*). Protection in $LAT1^{\Delta R\gamma t}$ mice was confirmed by analyzing keratinocyte proliferation by means of H&E and Ki-67 staining of skin sections, which was markedly reduced compared with that in $LAT1^{WT}$ mice (Fig 3, *B*). IMQ-treated $LAT1^{\Delta R\gamma t}$ mice also displayed decreased infiltration of neutrophils and monocyte-derived inflammatory macrophages compared with IMQ-treated $LAT1^{WT}$ mice (Fig 3, *C*). Importantly, lower numbers of dermal CD4 and γδ T-cell populations were observed in the dorsal skin of IMQ-treated $LAT1^{\Delta R\gamma t}$ mice compared with $LAT1^{WT}$ mice (Fig 3, *D*).

Analysis of draining lymphoid cells from IMQ-treated $LAT1^{WT}$ mice showed that IL-17–producing $CD27^-$ γδ T cells express LAT1 in contrast to $CD27^+$ γδ T cells, which do not secrete IL-17 (see Fig E3, *A*, in this article's Online Repository at www.jacionline.org). $LAT1^{\Delta R\gamma t}$ mice showed a reduced frequency of $CD27^-$ Tm^+ γδ T cells and lower Ki-67 expression than IMQ-treated $LAT1^{WT}$ mice (Fig 3, *E*). Moreover, application of IMQ increased expression of LAT1 in dermal $V\gamma4^+$ and $V\gamma4^-$ γδ T cells in $LAT1^{WT}$ mice (Fig 3, *F*). Similarly, LAT1 expression was mainly increased in $CD27^-$ $V\gamma4^+\delta4^+$ T cells detected in draining lymph nodes after IMQ application (Fig 3, *G*). These results indicate that deletion of LAT1 affected innate and adaptive lymphocyte expansion induced by IMQ, suggesting its potential role as a therapeutic target in skin inflammation. In addition, $LAT1^{\Delta R\gamma t}$ mice showed less ear thickness, S100A8/9 expression, and neutrophil and macrophage skin infiltration than $LAT1^{WT}$ mice (see Fig E3, *B-D*) in an alternative model of psoriasis induced by intradermal injection of IL-23.

Specific target deletion of LAT1 in CD4 T cells attenuates psoriasis

Although γδ T cells are essential to develop psoriasis in the IMQ- and IL-23–induced models,[8,10] this population is not the most abundant in patients with psoriasis, in which most of the IL-17–secreting cells are TCRαβ cells.[32] To determine whether specific deletion of LAT1 in CD4 T cells controls psoriasis development induced by IMQ, we crossed $LAT1^{fl/fl}$ mice with CD4-$Cre^{+/-}$ mice.[33] LAT1 deletion in CD4 T cells was confirmed by using Western blotting and FC analysis (see Fig E4, *A*, in this article's Online Repository at www.jacionline.org). *In vitro*–activated CD4 T cells from $LAT1^{\Delta CD4}$ mice showed reduced amino acid uptake compared with $LAT1^{WT}$ CD4 T cells (see Fig E4, *B*). Importantly, the specific inhibitor of LAT1, JPH203, completely blocked amino acid uptake in CD4 T cells, indicating the relevance of this specific essential amino acid transporter in CD4 T cells.

On treatment with IMQ, $LAT1^{\Delta CD4}$ mice displayed a smaller affected area and reduced redness and squamous appearance compared with $LAT1^{WT}$ mice (Fig 4, *A*). Histologic assessment revealed reduced epidermal thickness in $LAT1^{\Delta CD4}$ mice (Fig 4, *B*). Numbers of infiltrating neutrophils and CD4 T cells, but not $Ly6C^+$ macrophages and γδ T cells, were attenuated in the skin of $LAT1^{\Delta CD4}$ mice (Fig 4, *C* and *D*).

Expression of LAT1 was increased in CD4 T cells after IMQ application (Fig 4, *E*). Moreover, CD4 T-cell proliferation was induced by IMQ treatment in the lymph nodes of $LAT1^{WT}$ but not of $LAT1^{\Delta CD4}$ mice (Fig 4, *F*). As a control, we tested the proliferation of lymph node $CD27^-$ γδ T cells, which remained unaffected when LAT1 was deleted in CD4 T cells (see Fig E4, *C*). Transcriptional expression analysis of purified CD4 (Fig 4, *G*) and γδ (see Fig E4, *D*) T cells from the draining lymph nodes of mice treated with IMQ indicated that deletion of LAT1 in CD4 T cells specifically controls IL-17 mRNA levels in CD4 T cells but not in γδ T cells.

Transcriptional levels of IL-22 and IFN-γ in CD4 and γδ T cells after IMQ application were comparable between both genotypes (Fig 4, *G*, and see Fig E4, *D*). IL-10 expression was reduced in CD4 T cells from $LAT1^{\Delta CD4}$ mice compared with $LAT1^{WT}$ mice (Fig 4, *G*) but was similar in γδ T cells (see Fig E4, *D*). Expression of LAT1 mRNA levels was also increased by IMQ in CD4 T cells from $LAT1^{WT}$ mice (Fig 4, *G*).

Further stimulation with IL-23 and IL-1β of CD4 T cells purified from lymph nodes of IMQ-treated mice showed that $LAT1^{\Delta CD4}$ mice displayed lower levels of IL-17 and IL-22 expression (Fig 4, *H* and *I*). These data indicate that LAT1 controls expansion of CD4 T cells, as well as their ability to secrete IL-17 and IL-22 in response to IL-23 and IL-1β stimulation. Moreover, naive CD4 T cells from $LAT1^{\Delta CD4}$ and $LAT1^{WT}$ mice were differentiated *in vitro* toward the T_H17 program by means of addition of IL-6 and TGF-β in combination with IL-23 plus IL-1β. CD4 T cells from $LAT1^{\Delta CD4}$ mice displayed lower numbers of $IL\text{-}17^+$ cells and secreted less IL-17 and IL-22 than cells expressing LAT1 (see Fig E4, *E*). Human CD4 T cells from healthy donors were also *in vitro* differentiated toward T_H17 with the same cytokine cocktail

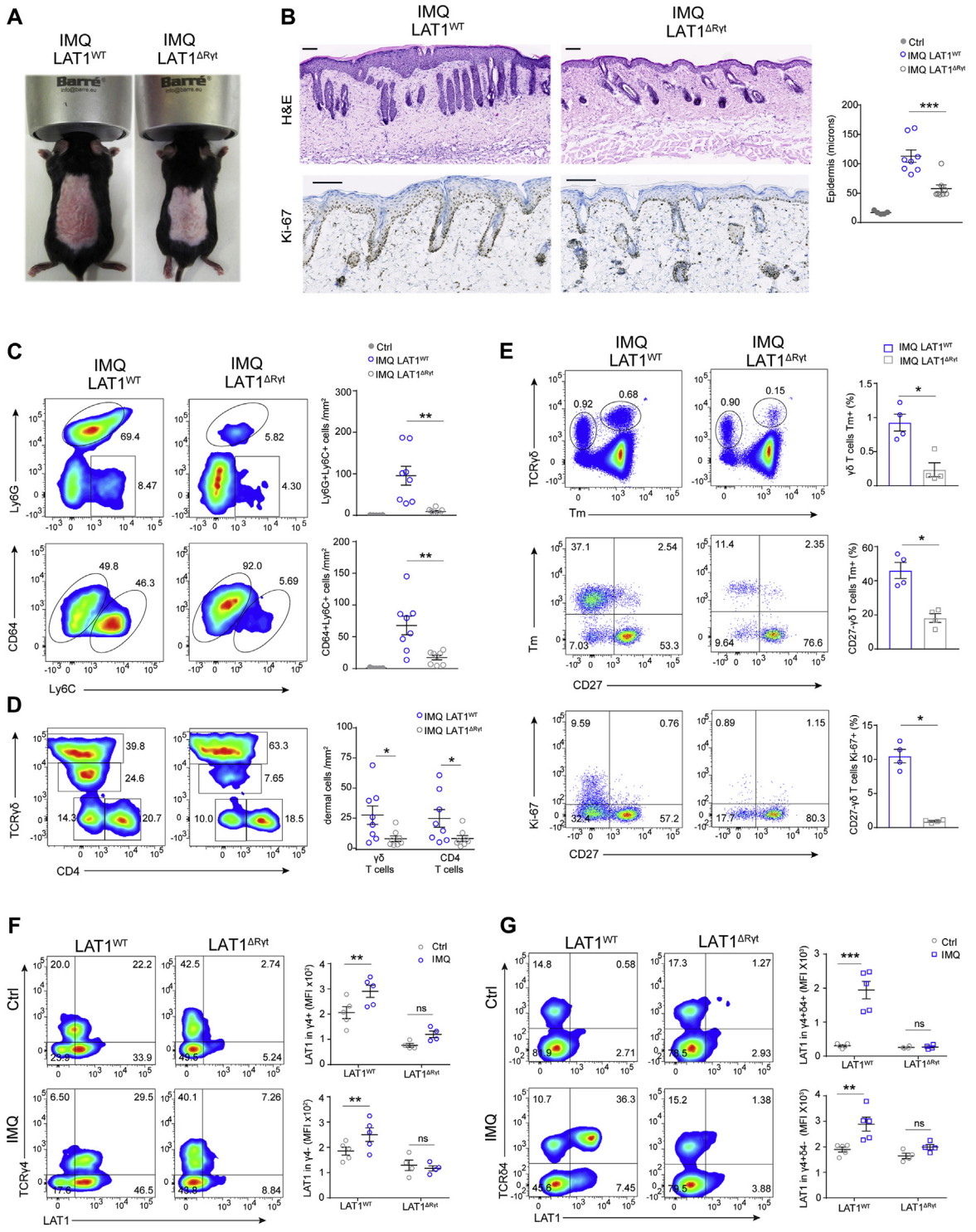

FIG 3. Deletion of LAT1 in innate and adaptive T cells prevents IMQ-induced psoriasis. **A,** Representative pictures of LAT1^{WT} and LAT1$^{\Delta R\gamma t}$ mice after IMQ. **B,** H&E-stained *(top)* and Ki-67–stained *(bottom)* sections. *Scale bars* = 100 μm. Averaged values of epidermal thickness are shown *(right)*. **C,** Skin neutrophils (Ly6G$^+$L6C$^+$; *upper*) and resident (CD64$^+$Ly6C$^-$) versus inflammatory macrophages (CD64$^+$Ly6C$^+$; *bottom*) were quantified. **D,** Dermal CD4 (*bottom* and *right*) and γδ T cells (*middle* and *left*) and epidermal γδ T cells (*upper* and *left*) were analyzed. Absolute numbers of cells are shown (Fig 3, *C* and *D*, *right*). **E,** Dot plots of Tm$^+$ γδ T cells from CD3$^+$ cells *(upper)*, Tm$^+$ CD27$^-$ cells *(middle)*, and CD27$^-$ γδ Ki-67$^+$ T cells *(bottom)* from total γδ T cells are shown. Frequency values are indicated *(right)*. **F** and **G,** LAT1 expression in Vγ4$^+$ *(top)* and Vγ4$^-$ *(bottom)* dermal T cells (Fig 3, *F*) and lymph node Vδ4$^+$ *(top)* and Vδ4$^-$ *(bottom)* T cells (Fig 3, *G*) in normal and IMQ-treated mice. Data are represented as means ± SEMs. Results of 2 independent experiments are represented as absolute numbers per square millimeter (Fig 3, *C*; n = 4). Individual data from one representative experiment of 2 were shown (Fig 3, *D-F*; n = 4-5). *ns*, Not significant. $^*P < .05$, $^{**}P < .01$, and $^{***}P < .001$, 1-way ANOVA (Fig 3, *C*) or 2-way ANOVA (Fig 3, *E* and *F*) with the Bonferroni *post hoc* test and the 2-tailed Mann-Whitney test (Fig 3, *D*).

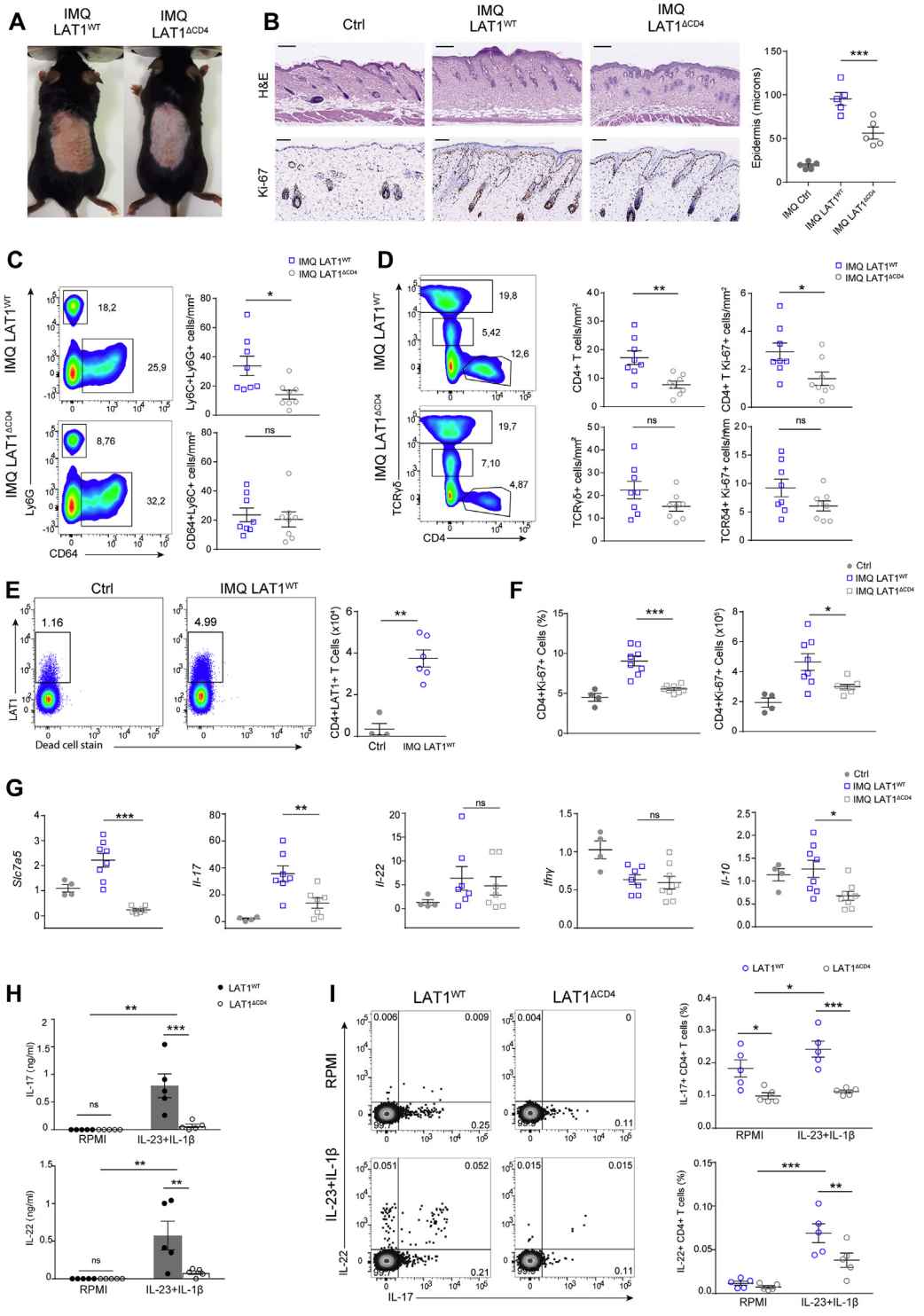

FIG 4. LAT1 expression in CD4 T cells contributes to development of IMQ-induced psoriasis. **A,** Representative pictures of IMQ-treated LAT1^{WT} and LAT1$^{\Delta CD4}$ mice. **B,** H&E-stained *(top)* and Ki-67–stained *(bottom)* sections. *Scale bars* = 100 μm. Averaged values of epidermal thickness are shown *(right)*. **C,** Skin neutrophil (Ly6G^{+}; *top*) and macrophage (CD64^{+}; *right*) quantification. **D,** Dermal CD4 (*right* and *bottom*) and γδ (*left* and *middle*) T cells and epidermal γδ T cells (*left* and *upper*) were analyzed. Total numbers *(left)* and Ki-67^{+} dermal CD4 and γδ T cells are shown *(right)*. **E,** LAT1 expression in CD4 T cells in lymph nodes. **F,** Frequencies *(left)* and absolute numbers *(right)* of CD4^{+}Ki-67^{+} cells in lymph nodes. **G,** Transcriptional expression in CD4 T cells after IMQ. **H** and **I,** Cytokines level (ELISA). **I,** Dot plots and frequencies of IL-17^{+} *(upper)* and IL-22^{+} *(lower)* CD4 T cells obtained from IMQ-treated mice and stimulated with IL-23 plus IL-1β and PMA/ionomycin. A pool of 2 independent experiments (Fig 4, *C*, *D*, *F*, and *G*) or data from one of 2 experiments (Fig 4, *E*, *H*, and *I*; n = 4-6) are shown. Data are shown as means ± SEMs. *ns*, Not significant. **P* < .05, ***P* < .01, and ****P* < .001, 2-tailed unpaired Student *t* test (Fig 4, *C-E*), 1-way ANOVA (Fig 4, *F* and *G*), or 2-way ANOVA (Fig 4, *H* and *I*) with the Bonferroni *post hoc* test.

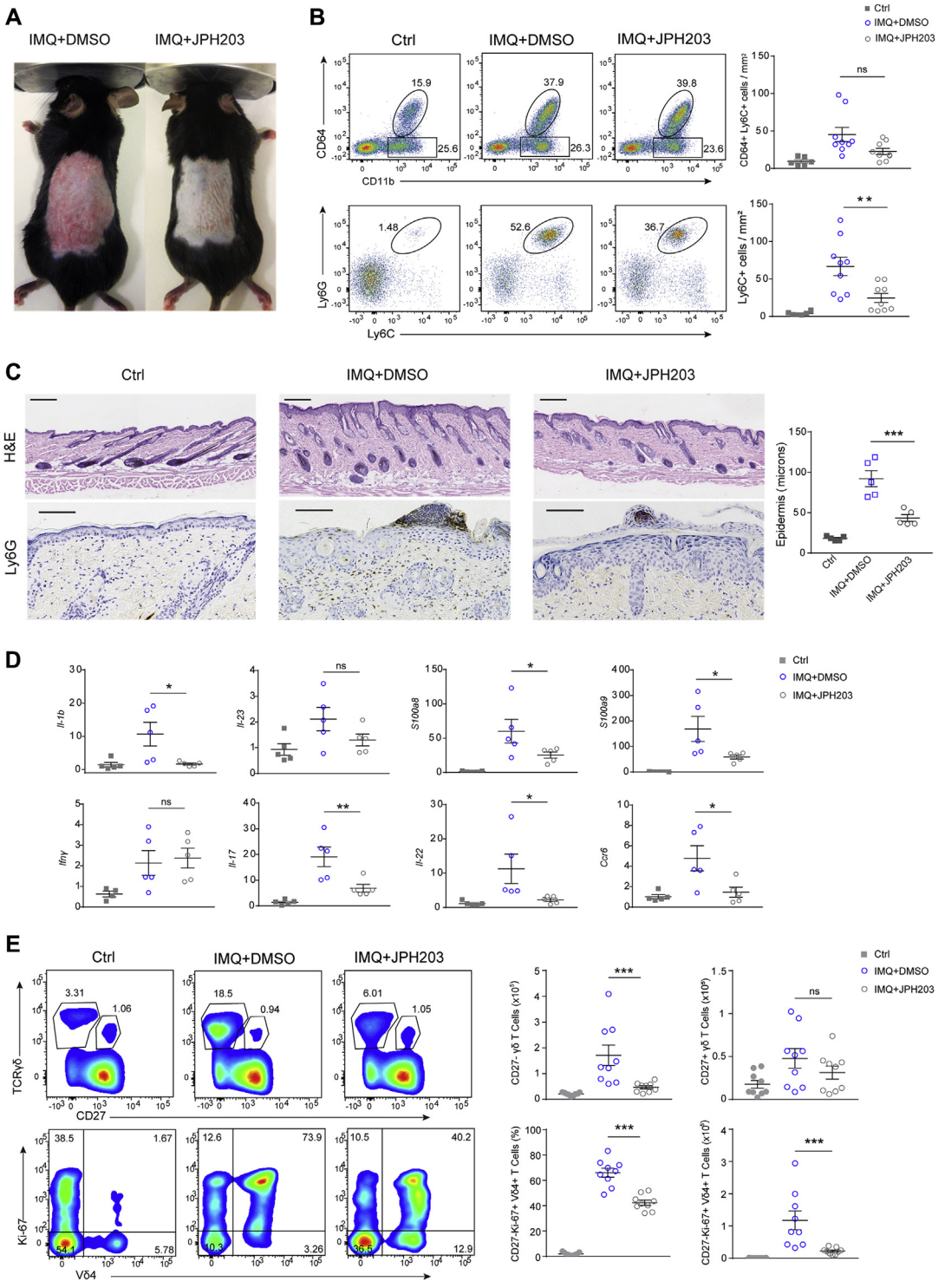

FIG 5. The inhibitor of LAT1, JPH203, prevents IMQ-induced skin inflammation. **A,** Representative pictures from mice treated with DMSO or JPH203 and topical application of IMQ. **B,** Dot plots identifying macrophages ($CD64^+CD11b^+$; *top*) and neutrophils ($Ly6G^+Ly6C^+$; *bottom*) in $CD45^+$ and $CD45^+CD64^-$ populations in the dorsal skin, respectively. Density values of macrophages and neutrophils are shown *(right)*. **C,** Representative H&E-stained *(top)* and Ly6G-stained *(bottom)* skin sections. *Scale bars* = 100 μm. Averaged values of epidermal thickness per mouse are shown in the graphic at right. **D,** Relative fold induction of indicated genes induced in the skin by IMQ. **E,** Representative density plots for $CD27^-$ and $CD27^+$ TCRγδ T cells in the $CD3^+$ gated population *(upper)* and frequencies of $V\delta4^+Ki\text{-}67^+$ cells on gated $CD27^-$ γδ T cells *(bottom)* in skin-draining lymph nodes. Absolute numbers or frequencies detected in cellular lymph node suspensions are shown per group *(right)*. A pool of 2 independent experiments (Fig 5, *B* and *E*) or data from one of 2 individual experiments (Fig 5, *D*) are shown (n = 4-5). Data are shown as means ± SEMs. *ns*, Not significant. $*P < .05$ and $**P < .01$, 1-way ANOVA with the Bonferroni *post hoc* test (Fig 5, *B*, *D*, and *E*).

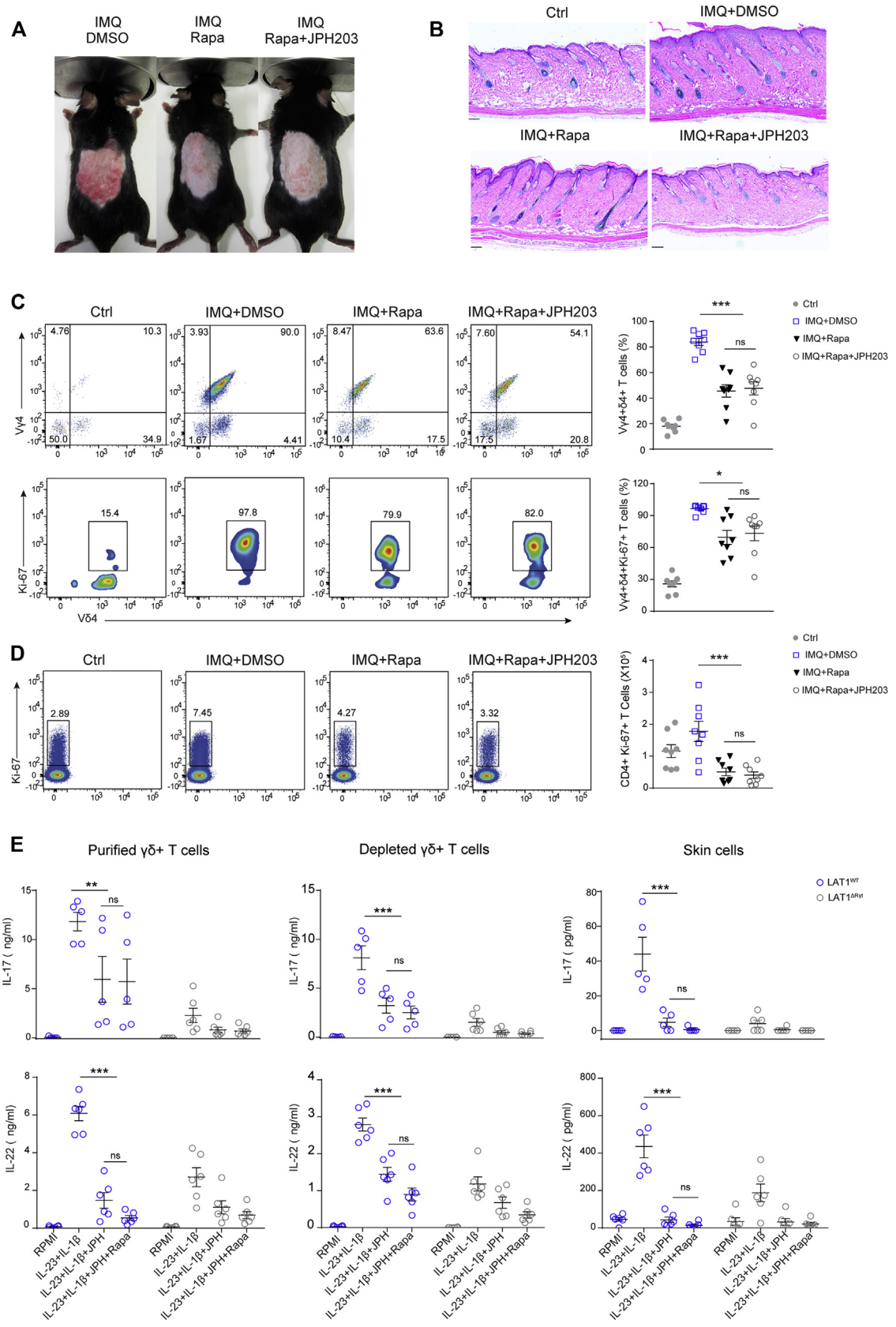

FIG 6. LAT1 acts as an upstream regulator of mTOR in the control of IMQ-induced psoriasis. **A,** Representative pictures of mice after 4 days of IMQ and treated with DMSO, rapamycin *(Rapa)*, or JPH203 plus rapamycin. **B,** Representative H&E-stained skin sections per group. *Scale bars* = 100 μm.

(see Fig E4, *F*). After 12 days in culture, stimulation with phorbol 12-myristate 13-acetate (PMA) and ionomycin confirmed that LAT1 inhibition controls secretion of IL-17 and IFN-γ in human CD4 T cells. These results indicate that LAT1 expression is necessary for human and mouse CD4 T_H1 and T_H17 polarization.

Pharmacologic inhibition of LAT1 prevents IMQ-induced psoriasis in mice

Mice were randomly treated with dimethyl sulfoxide (DMSO; vehicle) or LAT1 inhibitor (JPH203) to ascertain whether pharmacologic inhibition of LAT1 can affect IMQ-induced psoriasis severity. Inhibition of LAT1 during IMQ application caused a marked reduction of the appearance of psoriasis hallmarks, such as redness, epidermal thickening, and neutrophil infiltration (Fig 5, *A-C*).

To confirm the beneficial effect of JPH203 against psoriasis, we evaluated transcriptional levels of several proinflammatory mediators in the skin (Fig 5, *D*) and draining lymph nodes (see Fig E5, *A*, in this article's Online Repository at www.jacionline.org). JPH203 treatment prevented the increase in IL-1β, IL-17A, IL-22, S100A8, and S100A9 levels induced by IMQ in the skin (Fig 5, *D*). Interestingly, reduced transcriptional expression of CCR6 was also detected in the skin of JPH203-treated mice compared with that in DMSO-treated mice, which is consistent with a reduction in skin infiltration by IL-17–releasing cells.[34] In contrast, we found no difference in IL-23 and IFN-γ levels (Fig 5, *D*). These experiments also revealed reduced transcription of IL-17 and IL-22 in skin-draining lymph nodes from JPH203-treated mice (see Fig E5, *A*). However, transcriptional levels of IL-10, IFN-γ, CCL5, and CCL20 were comparable in both the JPH203- and DMSO-treated groups. Likewise, increased transcriptional levels of the LAT1 gene *(Slc7a5)* but not the CD98 gene *(Slc3a2)* were found in the lymph nodes of IMQ-treated mice supplemented with JPH203 or DMSO compared with the control group (see Fig E5, *A*).

Inhibition of LAT1-mediated amino acid transport prevented IMQ-induced expansion of γδ T cells in skin-draining lymph nodes, which mostly express γ4 and δ4 chains (Fig 5, *E*). A significant reduction in numbers of $CD27^-$ γδ T cells was detected in mice treated with JPH203 compared with the DMSO group, whereas the population of $CD27^+$ γδ T cells remained unaffected (Fig 5, *E*). $CD27^-$ $γ4^+δ4^+$ T cells displayed high levels of Ki-67, indicating that they actively proliferate in the DMSO-treated group, whereas their proliferation was significantly reduced in mice treated with JPH203. These data indicate that LAT1 inhibition controls $CD27^-$ γδ T-cell proliferation (Fig 5, *E*).

Moreover, the skin of mice treated with JPH203 contained fewer infiltrating $Vγ4^+δ4^+$ T cells than the skin of DMSO-treated mice (see Fig E5, *B*). Skin-infiltrating $Vγ4^+δ4^+$ T cells were mostly positive for Ki-67 in DMSO-treated mice, indicating their proliferative activity. Also, JPH203 significantly reduced the frequency of Ki-$67^+Vγ4^+δ4^+$ T cells in the skin (see Fig E5, *B*). In addition to its effect on γδ T cells, JPH203 also controlled the expansion of CD4 T cells (data not shown).

In summary, systemic administration of the LAT1 inhibitor JPH203 attenuates the skin response to IMQ by limiting the expression of most proinflammatory mediators as well, as the proliferation of CD4 and γδ T cells.

Human γδ T cells can be activated and expanded by phosphorylated antigens, such as zoledronate.[35] After 10 days, the presence of Ki-67^+ γδ T cells is greater than 85% (data not shown), but cotreatment with JPH203 significantly prevented their expansion (see Fig E5, *C*). Western blot analysis of human γδ T cells confirmed expression of the LAT1-CD98 complex (see Fig E5, *C*).

The LAT1/mTOR axis controls inflammatory responses in the IMQ-psoriasis model

To evaluate the role of mTOR activation in the control of CD4 and $Vγ4^+δ4^+$ T-cell expansion in mice with LAT1 deletion or inhibition, we assessed the effect of the mTOR inhibitor rapamycin alone or in combination with JPH203 (JPH203 plus rapamycin) during IMQ challenge. Mice treated with rapamycin or JPH203 plus rapamycin displayed reduced skin inflammation induced by IMQ (Fig 6, *A*) and reduced epidermal thickness (Fig 6, *B*). Rapamycin and JPH203 plus rapamycin caused a similar reduction in the frequency of $Vγ4^+δ4^+$ T cells detected in the draining lymph nodes (Fig 6, *C*). The fraction of $Vγ4^+δ4^+$ T cells expressing Ki-67 was reduced by rapamycin, but no additional inhibitory effect was caused by JPH203 (Fig 6, *C*). In addition, expansion of CD4 T cells induced by IMQ was prevented by rapamycin or JPH203 plus rapamycin (Fig 6, *D*). Overall, no additional effect was observed by treatment with JPH203 in mice in which we had already inhibited mTOR signaling in inflammatory cells, indicating that LAT1 might be upstream of the mTOR pathway.

We next assessed the role of the LAT1/mTOR axis in the control of IL-17 and IL-22 secretion after stimulation with IL-23 and IL-1β. Lymph node cells from $LAT1^{ΔRγt}$ and $LAT1^{WT}$ mice treated with IMQ were used to obtain separate fractions of purified γδ T cells and the remaining lymph node cells. Both fractions, as well as total ear cell suspensions, were *in vitro* stimulated with IL-23 plus IL-1β with or without JPH203 alone or together with rapamycin (Fig 6, *E*). Cells derived from IMQ-treated $LAT1^{ΔRγt}$ mice barely responded to IL-23 plus IL-1β stimulation (ie, they did not secrete IL-17 and IL-22), and the inhibitory effects observed with JPH203 and JPH203 plus rapamycin were significant only in cells expressing LAT1. In addition, no significant differences were detected between cells treated with JPH203 alone and those treated with JPH203 plus rapamycin (Fig 6, *E*), further indicating that LAT1 acts upstream of mTOR to control IL-17–related cytokine release.

C, Dot plots of $Vγ4^+δ4^+$ *(upper)* and density plots of Ki-$67^+δ4^+$ *(bottom)* from live $CD27^-$ γδ T cells quantified in the lymph nodes. **D,** Dot plots of frequencies of Ki-67^+ cells from CD4 T cells in the lymph nodes. Individual values per mouse of frequencies (Fig 6, *C*) and total cell counts (Fig 6, *D*) are shown at right. **E,** Purified γδ T cells *(left)*, lymph node cells depleted of γδ T cells *(middle)*, and skin cell suspensions *(right)* of IMQ-treated mice of indicated genotypes were *in vitro* stimulated (24 hours) with IL-23 plus IL-1β and incubated with indicated inhibitors. Individual values per mouse of cytokine levels detected in supernatants by means of ELISA are shown. A pool of 2 independent experiments (Fig 6, *C* and *D*) or data from one representative experiment of 2 (Fig 6, *E*) are shown (n = 4-6). Data are shown as means ± SEMs. *ns*, Not significant. $*P < .05$, $**P < .01$, and $***P < .001$, 1-way ANOVA with the Bonferroni *post hoc* test (Fig 6, *C-E*).

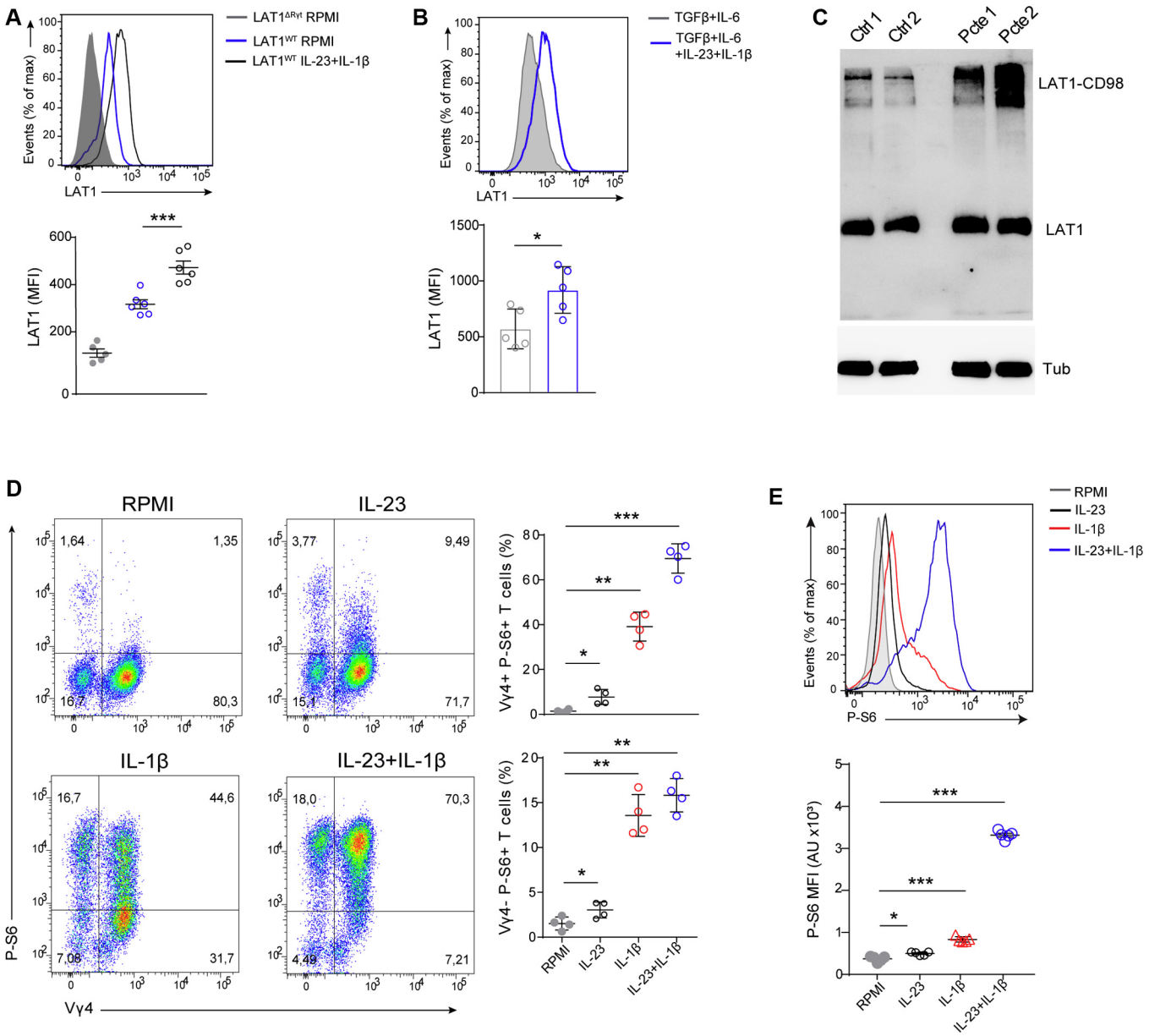

FIG 7. IL-23 and IL-1β upregulate LAT1 expression and induce mTOR activation in IL-17–secreting cells. **A** and **B,** Representative histograms *(upper)* and individual values *(bottom)* of LAT1 fluorescence in Vγ4$^+$ cells from lymph node cells of IMQ-treated mice (Fig 7, *A*) and *in vitro*–skewed T_H17 cells from WT mice (Fig 7, *B*) after IL-23 plus IL-1β stimulation. **C,** Peripheral CD4 T cells from healthy donors and patients with psoriasis were *in vitro* stimulated (48 hours) with IL-23 plus IL-1β. Expression of LAT1 and the LAT1-CD98 heterodimeric complex determined by using Western blotting are shown. **D,** Total lymph node γδ T cells from IMQ-treated WT mice were stimulated (24 hours) with IL-23, IL-1β, or both. Dot plots *(left)* and frequencies *(right)* of P-S6 expression in γ4$^+$ *(upper)* and γ4$^-$ *(bottom)* cells are shown. **E,** Histograms *(upper)* and values of fluorescence intensity for P-S6 expression *(bottom)* in the total fraction of CD27$^-$γ4$^+$ T cells stimulated as in Fig 7, *D*. A representative experiment of 2 individual replicates is shown (at least n = 5 [Fig 7, *A, B, D,* and *E*] and n = 2 [Fig 7, *C*] samples per group). Data are represented as means ± SEMs. *ns*, Not significant. **P* < .05 and ****P* < .001, 1-way ANOVA (Fig 7, *A, D,* and *E*) with the Bonferroni *post hoc* test and the 2-tailed paired Student *t* test (Fig 7, *B*).

LAT1 regulates the IL-23– and IL-1β–induced PI3K/AKT/mTOR pathway in IL-17–secreting cells

We further explored the mechanism through which LAT1 controls expansion of immune cells in psoriasis. A previous study proposed that AHR controls γδ T-cell proliferation in response to IMQ.[36] To address this, we inhibited LAT1 in AHR$^{+/-}$ and AHR$^{-/-}$ mice. JPH203 treatment dampened CD27$^-$ γδ and specifically Vγ4$^+$δ4$^+$ T-cell expansion in IMQ-treated AHR$^{+/-}$ and AHR$^{-/-}$ mice groups (see Fig E6, *A*, in this article's Online Repository at www.jacionline.org), indicating that the effect of LAT1 inhibition on γδ T-cell proliferation is largely independent of AHR expression. Moreover, JPH203 decreased the frequency and number of IL-17–secreting γδ T cells in both genotypes after IMQ challenge (see Fig E6, *B*).

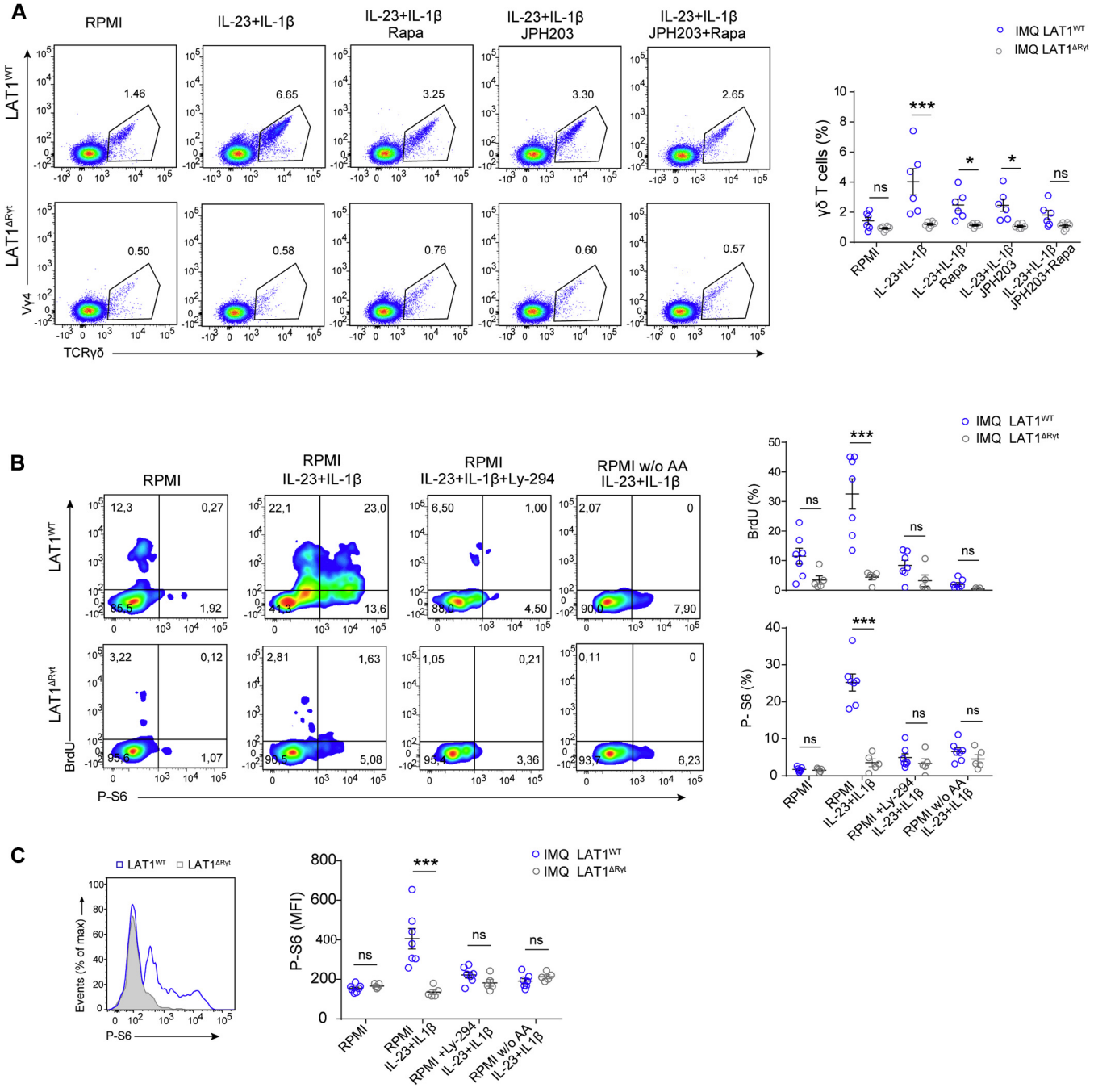

FIG 8. LAT1 is required to activate the PI3K/AKT/mTOR pathway induced by IL-23 and IL-1β to promote proliferation of IL-17–releasing cells. **A,** Lymph node cells from IMQ-treated mice were stimulated *in vitro* (48 hours) with the indicated cytokines and inhibitors. Dot plots *(left)* and individual values *(right)* of γδ T-cell frequencies from $CD3^+$ cells are shown. **B,** Density plots *(left)* and frequencies *(right)* of $BrdU^+$ and $P\text{-}S6^+V\gamma4^+$ cells obtained and stimulated as in Fig 7, *A*. **C,** Representative histogram of P-S6 expression *(left)* and individual values of P-S6 fluorescence *(right)* in $V\gamma4^+$ cells is shown. A representative experiment of 2 individual replicates is shown (at least n = 5). Data are shown as means ± SEMs. *ns*, Not significant. $^*P < .05$ and $^{***}P < .001$, 2-way ANOVA with the Bonferroni *post hoc* test.

To characterize the molecular triggers of LAT1 expression in psoriasis, we assessed the effect of the proinflammatory cytokines IL-23 and IL-1β. Both cytokines play crucial roles in T_H17 development[37] and promote extrathymic commitment of $IL\text{-}17^+$ γδ T cells in the IMQ model.[12] LAT1 expression was significantly increased by IL-23 plus IL-1β stimulation in $V\gamma4^+$ T cells from the lymph nodes of mice treated with IMQ (Fig 7, *A*). Stimulation with IL-23 and IL-1β also increased LAT1 expression of $CD4^+IL\text{-}17^+$ T cells differentiated *in vitro* (Fig 7, *B*). Moreover, peripheral CD4 T cells from patients with psoriasis expressed

high levels of LAT1-CD98 complex when stimulated with IL-23 plus IL-1β compared with cells from healthy donors (Fig 7, *C*). These results suggested that LAT1 is essential for the expansion of IL-17–secreting T lymphocytes induced by IL-23 and IL-1β.

IL-23 and IL-1β also induce activation of the mTOR pathway, as assessed by an increase in P-S6 detection, in γδ T cells (Fig 7, *D* and *E*). Remarkably, the combination of IL-23 plus IL-1β potentiates the effect of each cytokine alone on P-S6 activation in both $\gamma4^+$ and $\gamma4^-$ T cells (Fig 7, *D* and *E*).

Stimulation with IL-23 plus IL-1β induced expansion of $V\gamma4^+$ cells but only when LAT1 was expressed (Fig 8, *A*). However, expansion of $V\gamma4^+$ T cells from $LAT1^{WT}$ mice is reduced by addition of either mTOR or LAT1 inhibitors. These inhibitors had no effect on cells from $LAT1^{\Delta R\gamma t}$ mice (Fig 8, *A*). Finally, the combination of mTOR and LAT1 inhibitors had no additive effect, further confirming that LAT1 and mTOR are likely part of the same signaling pathway in these cells. The effects of IL-23 plus IL-1β stimulation in BrdU incorporation and S6 phosphorylation in $V\gamma4^+$ T cells were completely blocked by PI3K inhibitor (Ly294002) or by amino acid depletion (Fig 8, *B*). Cells from $LAT1^{\Delta R\gamma t}$ mice did not display mTOR activation or proliferation under any of the conditions assayed (Fig 8, *C*). These data indicate that IL-23 and IL-1β trigger LAT1 expression in $V\gamma4^+$ T cells and T_H17 cells, which promotes PI3K/AKT-induced mTOR signaling to control their expansion and IL-17 secretion.

DISCUSSION

The pathogenesis of psoriasis requires complex mechanisms that involve the interplay between keratinocytes and inflammatory cells.[1] Genetic studies aimed at identifying new genetic pathways associated with psoriasis risk demonstrated that alterations in metabolic pathways, such as those involved in transporting inorganic ions and amino acids, positively correlate with increased psoriasis risk.[38] Increased transcriptional levels of *Slc7a5* were detected in skin samples of patients with psoriasis.[22] The present study represents the first description of the increased expression of LAT1 protein in psoriatic lesions in keratinocytes and infiltrating lymphocytes. Pharmacologic inhibition of LAT1 effectively blocks skin inflammation induced in mice by means of IMQ application. The anti-inflammatory effects of the inhibitor can be recapitulated by genetic deletion of LAT1 in lymphocytes, including RORγt-expressing cells, such as γδ T cells and CD4 T cells.

The mTOR pathway is hyperactivated in keratinocytes from patients with psoriasis.[39] Its aberrant induction is mediated by proinflammatory cytokines, such as IL-1β, IL-17A, and TNF-α, increasing proliferation and reducing expression of differentiation markers.[40] Our results indicate that LAT1 expression in keratinocytes is not essential for control of keratinocyte proliferation, indicating a functional compensation with alternative amino acid transporters, such as LAT2 or LAT3, which are also expressed in the epidermal layer in patients with psoriasis.

A major feature of the IMQ model is expansion of $CD27^-\gamma4^+\delta4^+$ T cells in draining lymph nodes that produce IL-17.[12,28,41] A similar expansion of this population is observed in a mouse experimental autoimmune encephalomyelitis model.[42] Our results demonstrate that $IL\text{-}17^+\gamma4^+\delta4^+$ T-cell expansion after skin sensitization with IMQ is blocked by targeting LAT1 pharmacologically or genetically. Importantly, LAT1 inhibition also blocks expansion of human γδ T cells. Further experiments will address whether LAT1 deletion controls $\gamma4^+$ T-cell expansion in patients with other IL-17–mediated diseases, such as autoimmune encephalomyelitis.

LAT1 inhibition controls the proliferation of $V\gamma4^+\delta4^+$ T cells, even in the absence of AHR. However, LAT1 inhibition in the presence of the canonical mTOR inhibitor rapamycin had no additive effect. Inhibition of mTOR by targeting LAT1 could be an alternative approach to specifically target immune cells stimulated by IL-23 and IL-1β in patients with inflammatory diseases.

LAT1 deletion in dermal γδ T cells also effectively controls IL-23–induced skin inflammation. Nevertheless, the main disadvantage of IMQ- and IL-23–induced murine models of psoriasis is their dependence on γδ T cells.[8,10] Although the increased frequency of γδ T cells has been observed also in human psoriatic lesions,[2] their relevance in the onset or recurrence of disease is not clearly established.[43,44] Indeed, human psoriatic lesions show a greater frequency of IL-17–releasing $TCR\alpha\beta^+$ T cells than γδ T cells.[32] Our data demonstrate that LAT1 deletion in CD4 T cells dampens IMQ-induced skin inflammation. Moreover, LAT1 inhibition successfully impairs the T_H17 differentiation program in human CD4 T cells. Because the LAT1 inhibitor JPH203 is currently in clinical trials,[21] we propose that blocking LAT1-mediated amino acid transporter merits consideration as a novel immunosuppressive strategy to control the expansion of innate and adaptive T cells in the reactive state in patients with inflammatory diseases.

Whether mTOR activation is required for T_H17 cell expansion has been studied extensively[45]; however, the role of T_H17 driver cytokines, such as IL-23 and IL-1β, in mTOR activation had not been fully characterized. T_H17 cell development required TCR-mediated activation, which triggers the PI3K/AKT/mTOR signaling axis. LAT1 expression is induced after TCR engagement and is essential to properly activate αβ T cells.[17] LAT1 expression after TCR activation requires nuclear factor κ-light-chain-enhancer of activated B cells (NF-κB) and activator protein 1 activation.[46] The data herein clearly show that IL-23 and IL-1β stimulation also regulates LAT1 expression in T_H17 cells, as well as in γδ T cells, which do not receive TCR input.

IL-23–induced Janus kinase 2 activation triggers the PI3K/AKT and NF-κB pathways.[47] IL-1β stimulation can induce NF-κβ activation through myeloid differentiation response gene–88,[48] which is also essential for mTOR activation in T_H17 cells.[49] Moreover, IL-1R signaling induced PI3K/AKT phosphorylation and mTOR activation to promote differentiation of pathogenic T_H17 cells.[50] Our data indicate that inhibition of PI3K/AKT or amino acid depletion abrogated mTOR activation induced by IL-23 and IL-1β in γδ T cells. Importantly, PI3K/AKT signaling is important for expansion of IL-17–secreting γδ T cells.[51,52] Our data suggest that IL-23 and IL-1β induce LAT1 expression as a positive feedback loop to drive activation of that PI3K/AKT/mTOR pathway, which is essential for increased survival and expansion of IL-17–releasing cells.

LAT1 inhibition decreased transcriptional levels of IL-1β in the skin. This effect is potentially related to blockade of amino acid uptake in skin macrophages, which is also involved in IL-1β secretion.[53] This additional anti-inflammatory effect of JPH203 might contribute to prevention of psoriasis. However, genetic deletion of LAT1 in γδ and CD4 T cells was sufficient to control disease development.

This work provides the first evidence that murine psoriasis models can be precisely modulated by targeting inflammatory cell metabolism. Our data postulate that the LAT1 inhibitor JPH203, which has already been tested in patients with cancer for biosafety,[54] could be an alternative to control chronic skin inflammation.

We thank the CNIC facilities, especially the celomic, microscopy, and animal care–related personnel.

Key messages

- **LAT1 (SLC7A5) expression is increased in patients with psoriasis in both keratinocytes and dermal infiltrating lymphocytes, and its expression is upregulated by IL-23 and IL-1β.**
- **LAT1 inhibition does not affect keratinocyte proliferation but impairs expansion of IL-17–secreting γδ and CD4 T cells.**
- **LAT1 controls IL-23 plus IL-1β–induced PI3K/AKT/mTOR signaling in IL-17–secreting γδ and CD4 T cells to guarantee their expansion and cytokine secretion.**

REFERENCES

1. Hawkes JE, Chan TC, Krueger JG. Psoriasis pathogenesis and the development of novel targeted immune therapies. J Allergy Clin Immunol 2017;140:645-53.
2. Laggner U, Di Meglio P, Perera GK, Hundhausen C, Lacy KE, Ali N, et al. Identification of a novel proinflammatory human skin-homing Vgamma9Vdelta2 T cell subset with a potential role in psoriasis. J Immunol 2011;187:2783-93.
3. Villanova F, Flutter B, Tosi I, Grys K, Sreeneebus H, Perera GK, et al. Characterization of innate lymphoid cells in human skin and blood demonstrates increase of NKp44+ ILC3 in psoriasis. J Invest Dermatol 2014;134:984-91.
4. Kim J, Krueger JG. Highly effective new treatments for psoriasis target the IL-23/type 17 T cell autoimmune axis. Annu Rev Med 2017;68:255-69.
5. Yamanaka K, Mizutani H. "Inflammatory skin march": IL-1-mediated skin inflammation, atopic dermatitis, and psoriasis to cardiovascular events. J Allergy Clin Immunol 2015;136:823-4.
6. Beringer A, Noack M, Miossec P. IL-17 in Chronic inflammation: from discovery to targeting. Trends Mol Med 2016;22:230-41.
7. Keijsers RR, Joosten I, van Erp PE, Koenen HJ, van de Kerkhof PC. Cellular sources of IL-17 in psoriasis: a paradigm shift? Exp Dermatol 2014;23:799-803.
8. Cai Y, Shen X, Ding C, Qi C, Li K, Li X, et al. Pivotal role of dermal IL-17-producing gammadelta T cells in skin inflammation. Immunity 2011;35:596-610.
9. Rizzo HL, Kagami S, Phillips KG, Kurtz SE, Jacques SL, Blauvelt A. IL-23-mediated psoriasis-like epidermal hyperplasia is dependent on IL-17A. J Immunol 2011;186:1495-502.
10. Pantelyushin S, Haak S, Ingold B, Kulig P, Heppner FL, Navarini AA, et al. Rorγt+ innate lymphocytes and γδ T cells initiate psoriasiform plaque formation in mice. J Clin Invest 2012;122:2252-6.
11. Chung Y, Chang SH, Martinez GJ, Yang XO, Nurieva R, Kang HS, et al. Critical regulation of early Th17 cell differentiation by interleukin-1 signaling. Immunity 2009;30:576-87.
12. Muschaweckh A, Petermann F, Korn T. IL-1beta and IL-23 promote extrathymic commitment of CD27(+)CD122(-) γδ T cells to gammadeltaT17 cells. J Immunol 2017;199:2668-79.
13. Palacin M, Nunes V, Font-Llitjos M, Jimenez-Vidal M, Fort J, Gasol E, et al. The genetics of heteromeric amino acid transporters. Physiology (Bethesda) 2005;20:112-24.
14. Yan R, Zhao X, Lei J, Zhou Q. Structure of the human LAT1-4F2hc heteromeric amino acid transporter complex. Nature 2019;568:127-30.
15. Wagner CA, Lang F, Broer S. Function and structure of heterodimeric amino acid transporters. Am J Physiol Cell Physiol 2001;281:C1077-93.
16. Taylor PM. Role of amino acid transporters in amino acid sensing. Am J Clin Nutr 2014;99:223S-30S.
17. Sinclair LV, Rolf J, Emslie E, Shi YB, Taylor PM, Cantrell DA. Control of amino-acid transport by antigen receptors coordinates the metabolic reprogramming essential for T cell differentiation. Nat Immunol 2013;14:500-8.
18. Loftus RM, Assmann N, Kedia-Mehta N, O'Brien KL, Garcia A, Gillespie C, et al. Amino acid-dependent cMyc expression is essential for NK cell metabolic and functional responses in mice. Nat Commun 2018;9:2341.
19. Hayase S, Kumamoto K, Saito K, Kofunato Y, Sato Y, Okayama H, et al. L-type amino acid transporter 1 expression is upregulated and associated with cellular proliferation in colorectal cancer. Oncol Lett 2017;14:7410-6.
20. Shimizu A, Kaira K, Kato M, Yasuda M, Takahashi A, Tominaga H, et al. Prognostic significance of L-type amino acid transporter 1 (LAT1) expression in cutaneous melanoma. Melanoma Res 2015;25:399-405.
21. Hayashi K, Anzai N. Novel therapeutic approaches targeting L-type amino acid transporters for cancer treatment. World J Gastrointest Oncol 2017;9:21-9.
22. Cibrian D, Saiz ML, de la Fuente H, Sanchez-Diaz R, Moreno-Gonzalo O, Jorge I, et al. CD69 controls the uptake of L-tryptophan through LAT1-CD98 and AhR-dependent secretion of IL-22 in psoriasis. Nat Immunol 2016;17:985-96.
23. van der Fits L, Mourits S, Voerman JS, Kant M, Boon L, Laman JD, et al. Imiquimod-induced psoriasis-like skin inflammation in mice is mediated via the IL-23/IL-17 axis. J Immunol 2009;182:5836-45.
24. Hirano K, Uno K, Kuwabara H, Kojima K, Ohno S, Sakurai H, et al. Expression of L-type amino acid transporter 1 in various skin lesions. Pathol Res Pract 2014;210:634-9.
25. Tina E, Prosen S, Lennholm S, Gasparyan G, Lindberg M, Gothlin Eremo A. Expression profile of the amino acid transporters SLC7A5, SLC7A7, SLC7A8 and the enzyme TDO2 in basal cell carcinoma. Br J Dermatol 2019;180:130-40.
26. Tarutani M, Itami S, Okabe M, Ikawa M, Tezuka T, Yoshikawa K, et al. Tissue-specific knockout of the mouse Pig-a gene reveals important roles for GPI-anchored proteins in skin development. Proc Natl Acad Sci U S A 1997;94:7400-5.
27. Madisen L, Zwingman TA, Sunkin SM, Oh SW, Zariwala HA, Gu H, et al. A robust and high-throughput Cre reporting and characterization system for the whole mouse brain. Nat Neurosci 2010;13:133-40.
28. Ramirez-Valle F, Gray EE, Cyster JG. Inflammation induces dermal Vγ4+ γδT17 memory-like cells that travel to distant skin and accelerate secondary IL-17-driven responses. Proc Natl Acad Sci U S A 2015;112:8046-51.
29. Eberl G, Littman DR. Thymic origin of intestinal αβ T cells revealed by fate mapping of RORγt+ cells. Science 2004;305:248-51.
30. Serre K, Silva-Santos B. Molecular mechanisms of differentiation of murine pro-inflammatory γδ T cell subsets. Front Immunol 2013;4:431.
31. Guo Y, MacIsaac KD, Chen Y, Miller RJ, Jain R, Joyce-Shaikh B, et al. Inhibition of RORγT skews TCRα gene rearrangement and limits T cell repertoire diversity. Cell Rep 2016;17:3206-18.
32. Matos TR, O'Malley JT, Lowry EL, Hamm D, Kirsch IR, Robins HS, et al. Clinically resolved psoriatic lesions contain psoriasis-specific IL-17-producing alpha-beta T cell clones. J Clin Invest 2017;127:4031-41.
33. Sawada S, Scarborough JD, Killeen N, Littman DR. A lineage-specific transcriptional silencer regulates CD4 gene expression during T lymphocyte development. Cell 1994;77:917-29.
34. Brucklacher-Waldert V, Steinbach K, Lioznov M, Kolster M, Holscher C, Tolosa E. Phenotypical characterization of human Th17 cells unambiguously identified by surface IL-17A expression. J Immunol 2009;183:5494-501.
35. Kondo M, Sakuta K, Noguchi A, Ariyoshi N, Sato K, Sato S, et al. Zoledronate facilitates large-scale ex vivo expansion of functional gammadelta T cells from cancer patients for use in adoptive immunotherapy. Cytotherapy 2008;10:842-56.
36. Cochez PM, Michiels C, Hendrickx E, Van Belle AB, Lemaire MM, Dauguet N, et al. AhR modulates the IL-22-producing cell proliferation/recruitment in imiquimod-induced psoriasis mouse model. Eur J Immunol 2016;46:1449-59.
37. Sallusto F, Zielinski CE, Lanzavecchia A. Human Th17 subsets. Eur J Immunol 2012;42:2215-20.
38. Aterido A, Julia A, Ferrandiz C, Puig L, Fonseca E, Fernandez-Lopez E, et al. Genome-wide pathway analysis identifies genetic pathways associated with psoriasis. J Invest Dermatol 2016;136:593-602.
39. Buerger C. Epidermal mTORC1 signaling contributes to the pathogenesis of psoriasis and could serve as a therapeutic target. Front Immunol 2018;9:2786.
40. Buerger C, Shirsath N, Lang V, Berard A, Diehl S, Kaufmann R, et al. Inflammation dependent mTORC1 signaling interferes with the switch from keratinocyte proliferation to differentiation. PLoS One 2017;12:e0180853.
41. Hartwig T, Pantelyushin S, Croxford AL, Kulig P, Becher B. Dermal IL-17-producing gammadelta T cells establish long-lived memory in the skin. Eur J Immunol 2015;45:3022-33.
42. Papotto PH, Goncalves-Sousa N, Schmolka N, Iseppon A, Mensurado S, Stockinger B, et al. IL-23 drives differentiation of peripheral gammadelta17 T cells from adult bone marrow-derived precursors. EMBO Rep 2017;18:1957-67.

43. Nishimoto S, Kotani H, Tsuruta S, Shimizu N, Ito M, Shichita T, et al. Th17 cells carrying TCR recognizing epidermal autoantigen induce psoriasis-like skin inflammation. J Immunol 2013;191:3065-72.
44. Di Meglio P, Villanova F, Navarini AA, Mylonas A, Tosi I, Nestle FO, et al. Targeting CD8(+) T cells prevents psoriasis development. J Allergy Clin Immunol 2016;138:274-276, e6.
45. Jones RG, Pearce EJ. MenTORing immunity: mTOR signaling in the development and function of tissue-resident immune cells. Immunity 2017;46:730-42.
46. Hayashi K, Jutabha P, Endou H, Sagara H, Anzai N. LAT1 is a critical transporter of essential amino acids for immune reactions in activated human T cells. J Immunol 2013;191:4080-5.
47. Cho ML, Kang JW, Moon YM, Nam HJ, Jhun JY, Heo SB, et al. STAT3 and NF-kappaB signal pathway is required for IL-23-mediated IL-17 production in spontaneous arthritis animal model IL-1 receptor antagonist-deficient mice. J Immunol 2006;176:5652-61.
48. Andreakos E, Sacre SM, Smith C, Lundberg A, Kiriakidis S, Stonehouse T, et al. Distinct pathways of LPS-induced NF-kappa B activation and cytokine production in human myeloid and nonmyeloid cells defined by selective utilization of MyD88 and Mal/TIRAP. Blood 2004;103:2229-37.
49. Chang J, Burkett PR, Borges CM, Kuchroo VK, Turka LA, Chang CH. MyD88 is essential to sustain mTOR activation necessary to promote T helper 17 cell proliferation by linking IL-1 and IL-23 signaling. Proc Natl Acad Sci U S A 2013;110:2270-5.
50. Deason K, Troutman TD, Jain A, Challa DK, Mandraju R, Brewer T, et al. BCAP links IL-1R to the PI3K-mTOR pathway and regulates pathogenic Th17 cell differentiation. J Exp Med 2018;215:2413-28.
51. Roller A, Perino A, Dapavo P, Soro E, Okkenhaug K, Hirsch E, et al. Blockade of phosphatidylinositol 3-kinase PI3Kdelta or PI3Kgamma reduces IL-17 and ameliorates imiquimod-induced psoriasis-like dermatitis. J Immunol 2012;189:4612-20.
52. Duan J, Chung H, Troy E, Kasper DL. Microbial colonization drives expansion of IL-1 receptor 1-expressing and IL-17-producing γ/δ T cells. Cell Host Microbe 2010;7:140-50.
53. Yoon BR, Oh YJ, Kang SW, Lee EB, Lee WW. Role of SLC7A5 in metabolic reprogramming of human monocyte/macrophage immune responses. Front Immunol 2018;9:53.
54. Okano N, Kawai K, Yamauchi Y, Kobayashi T, Naruge D, Nagashima F, et al. First-in-human phase I study of JPH203 in patients with advanced solid tumors. J Clin Oncol 2018;36(suppl):419.

METHODS

Chemical reagents

The LAT1-specific inhibitor JPH203, (S)-2-amino-3-(4-((5-amino-2-phenylbenzo [d] oxazol-7-yl) methoxy)-3,5-dichlorophenyl) propanoic acid, was purchased from MedKoo Biosciences (Morrisville, NC). All other reagents were purchased from Sigma (St Louis, Mo), unless otherwise indicated.

Mice

Mice were bred and maintained in the specific pathogen–free animal facilities of Centro Nacional de Investigaciones Cardiovasculares (Madrid, Spain). All animal experiments were performed in accordance with protocols approved by the institutional animal care committee and were approved by local and European ethics committees. For all experiments, we used littermates derived from crossing Cre-negative $Slc7a5^{fl/fl}$ $tomato^{fl/wt}$ female mice with Cre-positive $Slc7a5^{fl/wt}$ $tomato^{fl/wt}$ male mice. $LAT1^{WT}$ mice are $Cre^{+/-}Slc7a5^{fl/wt}Tomato^{fl/wt}$ mice, and $LAT1^{\Delta}$ mice are $Cre^{+/-}Slc7a5^{fl/fl}Tomato^{fl/wt}$ mice. K5-CreERT2 mice were kindly provided by Erwin Wagner (Medical University, Vienna, Austria). Mice (4 weeks) were fed with a 400-ppm tamoxifen diet (TD55125; Envigo, Indianapolis, Ind) for induction of Cre protein in the skin. $AHR^{-/-}$ mice were kindly provided by Pedro Salguero (Universidad de Extremadura, Badajoz, Spain). $AHR^{-/-}$ mice and their control littermate $AHR^{+/-}$ mice were obtained by breeding heterozygous parents. Forkhead box P3–mRFP reporter mice backcrossed with IL-17–green fluorescent protein reporter mice were kindly provided by Richard A. Flavell (Yale University, New Haven, Conn) and used as normal (WT) mice for experiments with either JPH203 or rapamycin inhibitors. All mouse strains used are on the C57BL/6 background. Experiments were conducted with male mice (8-12 weeks) kept on a regular 12-hour light/dark cycle (7 AM-7 PM light period), with food and water available *ad libitum*.

Human subjects

Patients with moderate-to-severe psoriasis who were recruited for the study had a Psoriasis Area and Severity Index of 8.0 or greater and washout periods of at least 14 days for topical corticosteroids and any systemic therapy. Skin punch biopsy specimens (3 mm) were obtained from patients with lesion plaque–type psoriasis and healthy volunteers. Blood samples (10 mL) were also collected from patients with psoriasis and healthy volunteers. The study was approved by the Hospital Universitario de La Princesa ethics committee, and all participants provided written informed consent.

Psoriasis model induction and treatment

Induction of local psoriasis-like inflammation on ear skin was done through daily topical administration of 10 mg of IMQ cream (5%) in each ear for 4 or 5 days. For systemic psoriasis induction, mice were mostly treated daily on shaved and depilated back skin with 50 mg of IMQ cream for 4 or 5 days. Exceptionally, $LAT1^{\Delta CD4}$ mice received 20 mg of IMQ daily on back skin for 8 days. When indicated, mice received daily doses of JPH203 (50 mg/kg of body weight) and rapamycin (5 mg/kg of body weight) dissolved in DMSO (through the intraperitoneal route) during the course of IMQ treatment. Mice without IMQ or treatment application are always included as a control group. The IL-23 model of psoriasis was conducted, as previously described.[E1] At least 10 intradermal injections of recombinant mouse IL-23 (500 ng in 20 μL of PBS; eBioscience, San Diego, Calif) were performed per mouse on alternate days. When indicated, mice received an injection of 50 μL (250 μg) of Brefeldin A (Sigma) dissolved in ethanol (5 mg/mL) and administered intraperitoneally 12 hours before death. For *in vivo* BrdU labeling of cells, 1 mg of BrdU dissolved in 100 μL of PBS was injected intraperitoneally 3 hours before mice were killed.

Skin analysis and staining

For histologic analysis, paraformaldehyde-fixed, paraffin-embedded dorsal skin sections were prepared and stained with H&E. At least 3 skin sections (3-5 μm) 300 μm apart from each other were analyzed per mouse. For quantification of epidermal thickness, at least 10 measurements, randomly performed between all sections, were averaged per mouse. For immunohistochemical staining, skin sections were deparaffinized, boiled in the suggested antigen retrieval solution, and incubated with the primary antibodies indicated in Table E1. Slides were developed with diaminobenzidene substrate (K3468; Dako, Glostrup, Denmark) and then counterstained with Mayer hematoxylin. For immunofluorescence of LAT1 in mice, fresh skin fragments were embedded in OCT compound. IL-17–green fluorescent protein was detectable in unfixed skin sections without staining.

Human skin sections were deparaffinized, boiled in the suggested antigen retrieval solution, blocked with BSA solution (2%), and incubated with the primary antibodies indicated in Table E1 for 18 hours at 4°C. The secondary antibodies used were the EnVision FLEX system for immunohistochemistry detection of LAT1/LAT2 (Dako) and Alexa Fluor 647–labeled chicken anti-rabbit for LAT1/LAT2 and LAT3 immunofluorescences. Nuclei were counterstained with 4′-6-diamidino-2-phenylindole dihydrochloride. Pictures were taken with a Zeiss LSM confocal microscope (Zeiss, Oberkochen, Germany) and analyzed with LSM image browser software.

Lymphocytes and skin cell preparations for FC

Tissues were dissected and grated through a nylon mesh (70-μm; BD Biosciences, San Jose, Calif) to obtain single-cell suspensions from peripheral lymph nodes. RBC lysis was performed with BD Pharm Lyse Buffer (BD Biosciences). Ears were split into dorsal and ventral halves, and dorsal skin was cut into small pieces. Tissues were digested for 30 minutes at 37°C in RPMI containing penicillin-streptomycin, HEPES buffer, 83 μg/mL Liberase (Roche Applied Science, Mannheim, Germany), 100 μg/mL DNAse I (Sigma), and 0.5 mg/mL Collagenase IV (Sigma) under constant stirring. Digestion enzymes were quenched by addition of 5 mmol/L EDTA and 0.5% BSA. Undigested tissue was homogenously disaggregated with 7-mm stainless steel beads (Life Technologies, Grand Island, NY) in a TissueLyser LT (Qiagen, Hilden, Germany), one 3-minute cycle (20 osc/sec). Isolated skin cells were flowed through a 70-μm nylon filter (BD Biosciences). For analysis of keratinocytes, dorsal skin from mice treated or not with IMQ was incubated with 4 U/mL Dispase II (Roche) in MEM medium by 24 hours at 4°C. True count beads (BD Biosciences) were added to cell suspensions to quantify the total number of cells in further FC.

FC

Single-cell suspensions were incubated with Fc-blocking antibodies and subsequently stained with 1:200 dilutions of the appropriated surface marker antibodies detailed in Table E1. The staining panels always included dead cell staining with Fixable Yellow Viability Dye (Molecular Probes, Eugene, Ore). BrdU detection was performed according to the manufacturer's protocol (BD PharMingen). P-S6 (Ser235/236) (pS6) and Ki-67 staining were conducted with the FOXP3 Transcription Factor Staining Buffer Set (eBioscience) and with directed labeled antibodies against Ki-67 (B56; BD Biosciences) and pS6 (D57.2.2E; Cell Signaling, Danvers, Mass). For LAT1 and LAT2 detection, cells were fixed and permeabilized with Cytofix/Cytoperm Kit (BD Biosciences), and Alexa Fluor 647–labeled chicken anti-rabbit was used as a secondary antibody. A customized rabbit anti-mouse LAT2 (kindly provided by Dr Manuel Palacín, IRB, Barcelona, Spain) was used. Further description of antibodies is included in Table E1.

After staining, cells were washed and analyzed with FACSCanto or LSRFortessa (BD Biosciences). Data were further analyzed with FlowJo10 software (TreeStar, Ashland, Ore).

In vitro cultures and cytokine detection

Mouse cells were cultured in RPMI or Iscove modified Dulbecco medium supplemented with FCS (5%), 25 mmol/L HEPES, antibiotics, sodium pyruvate, and β-mercaptoethanol. When indicated, cells were incubated in

RPMI 1640 medium without amino acids and supplemented with normal FCS (5%; United States Biological, Salem, Mass). Naive CD4 T cells were purified from lymph nodes by using commercial kits (STEMCELL Technologies, Vancouver, British Columbia, Canada).

Naive CD4 T cells were seeded (1×10^6 cells/mL) in a 24-well plate coated with 5 μg/mL anti-CD3 (145 2C11; Tonbo Biosciences, San Diego, Calif) for 48 hours to test LAT1 expression and amino acid uptake experiments. For *in vitro* differentiation studies, naive CD4 T cells were seeded (1×10^6 cells/mL) in supplemented Iscove modified Dulbecco medium in 24-well plates coated with 5 μg/mL anti-CD3 (145 2C11) and 1 μg/mL anti-CD28 (37.51) antibodies (Tonbo Biosciences) and steered toward the T_H17 lineage with IL-6 (50 ng/mL), IL-23 (10 ng/mL), IL-1β (10 ng/mL), and TGF-β (1 ng/mL) for 4 days. When indicated, the T_H17 cells were cultured with IL-6 and TGF-β for 4 days at concentrations indicated previously, and stimulation with IL-23 and IL-1β was tested only by 24 hours.

Total CD4 T cells purified from $LAT1^{WT}$ and $LAT1^{\Delta CD4}$ mice after IMQ application were incubated by 18 to 24 hours with IL-23 and IL-1β cytokines (10 ng/mL each) to stimulate secretion of cytokines and P-S6 induction or 48 hours to assess proliferation. Similarly, cell suspensions from lymph nodes of $LAT1^{WT}$ and $LAT1^{\Delta R\gamma t}$ mice after IMQ application were split into 2 fractions: one was subjected to γδ T-cell depletion using anti-TCRγδ (clone GL3), and the other was used to purify γδ T cells with the EasySep Mouse Selection Kit (STEMCELL Technologies). The resulting fractions (purified γδ and γδ depleted) were *in vitro* stimulated by 18 to 24 hours with IL-23 and IL-1β to assess cytokine release by means of ELISA. Ear cell suspensions after IMQ application were also *in vitro* stimulated with IL-23 and IL-1β to assess cytokine release. Supernatants were collected, and IL-17 and IL-22 levels were assessed by using mouse ELISA Ready-SET-Go Kits (Fisher Scientific, Waltham, Mass). CD4 T cells were further stimulated with PMA (50 ng/mL; Sigma), ionomycin (1 mg/mL; Sigma-Aldrich), and brefeldin A (GolgiStop, 1 μg/mL; BD Biosciences) at 37°C in a 10% CO_2 atmosphere for 4 hours. After staining of surface markers, cells were fixed and permeabilized (Cytofix/Cytoperm and Perm/Wash Buffer; BD Biosciences), followed by staining with mAbs to mouse IL-17A and IL-22 (eBioscience). True count beads (BD Biosciences) were added to *in vitro* cultures to quantify the total number of expanded γδ T cells. Rapamycin (1 μmol/L), LY294002 (10 μmol/L), and JPH203 (10 μmol/L) inhibitors were added to the cultures when indicated. When indicated, BrdU at a final concentration of 5 μmol/L was added to assess proliferation according to the instructions of the BrdU Flow Kits (BD Life Science-Bioscience).

PBMCs from healthy donors were obtained, and CD4 T cells were isolated by using the EasySep Human CD4 T Cell Isolation Kit (STEMCELL Technologies). For T_H17 differentiation, isolated CD4 T cells were cultured for 12 days in RPMI 1640 medium supplemented with FCS (5%), 25 mmol/L HEPES, antibiotics, and sodium pyruvate with anti-CD3 (5 μg/mL; catalog no. 300314, RRID:AB314050; BioLegend) plus anti-CD28 mAbs (2 μg/mL; catalog no. 555725; BD). The following combination of cytokines and blocking antibodies was appropriate for T_H17 polarization: rhIL-6 and IL-1β (10 ng/mL), rhIL-23 (20 ng/mL), rhTGF-β1 (2 ng/mL), anti–IFN-γ (10 μg/mL), and anti–IL-4 (10 μg/mL; all cytokines from R&D Systems, Minneapolis, Minn) were added each 48 hours. JPH203 at 10 μmol/L or DMSO was also added to the culture on alternate days. At day 12, cells were further stimulated by 4 hours with PMA (50 ng/mL; Sigma) and ionomycin (1 mg/mL; Sigma-Aldrich) in the presence of brefeldin A (GolgiStop, 1 μg/mL; BD Biosciences). Fixed and permeabilized cells (Cytofix/Cytoperm and Perm/Wash Buffer; BD Biosciences) were stained with anti–IL-17 (BL168) and anti–IFN-γ (B27) antibodies (BioLegend) and analyzed in a FACScanto cytometer.

For expansion of human γδ T cells, total human PBMCs (10^6 cells/mL) from heathy donors (buffy coats) were stimulated in a 24-well plate in culture medium EX-VIVO 15 (Lonza, Bornem, Belgium) and expanded with zoledronic acid (5 μmol/L), as previously reported.[E2] At day 2, IL-2 (100 U/mL) and JPH203 inhibitor (10 μmol/L) were added and then replaced every 48 hours. At day 10, the number of Ki-67^+CD27^- γδ T cells was analyzed in a FACSCanto cytometer. LAT1 expression associated with CD98 was also confirmed in expanded (10 days) human γδ T cells by means of Western blotting.

RNA extraction and quantitative PCR analysis

Tissue total RNA was isolated with TRI Reagent (Sigma) or the Qiagen RNeasy Kit (Qiagen). Residual DNA contamination was removed with the Turbo DNA-free Kit (Ambion, Thermo Fisher, Waltham, Mass). Total RNA (200-1000 ng) was reverse transcribed to cDNA with a Reverse Transcription Kit (Applied Biosystems, Foster City, Calif). Quantitative PCR was then performed in an AB7900_384 (Applied Biosystems) by using SYBR Green (Applied Biosystems) as a reporter. Gene-specific primers used are listed in Table E2. Expression of each gene of interest was normalized to at least 2 housekeeping genes: β-actin *(ACTB)* and glyceraldehyde-3-phosphate dehydrogenase *(GAPDH)*. Data are presented as averaged relative fold differences calculated by using the $2^{-\Delta\Delta Ct}$ method with average values of healthy mice as a reference.

Western blotting

CD4 T cells from $LAT1^{\Delta R\gamma t}$ and $LAT1^{\Delta CD4}$ mouse cell lines were cultured (1×10^6 cells/mL) in RPMI medium for 24 hours in the presence of anti-CD3 (5 μg/mL). After lysis with RIPA buffer supplemented with protease and phosphatase inhibitor cocktails (Roche), lysates were separated by using SDS-PAGE and immunoblotted with anti-LAT1 antiserum (kindly provided by Dr P. Taylor, Dundee, United Kingdom).[E3] The loading control was carried out with a rabbit anti-mouse SMC protein 1A antibody (A300-055A; Bethyl Laboratories, Montgomery, Tex).

γδ T cells from PBMCs of patients with psoriasis were purified with the EasySep Human Gamma Delta T Cell Isolation Kit (STEMCELL Technologies) after 7-10 days in culture with zoledronate. CD4 T cells purified from PBMCs of patients with psoriasis or healthy volunteers were stimulated with anti-CD3 (2 μg/mL), anti-CD28 (1 μg/mL), IL-23 (20 ng/mL), and IL-1β (20 ng/mL) for 48 hours. Lysates of human γδ T cells and CD4 T cells were done with RIPA buffer, separated by using SDS-PAGE, and immunoblotted with rabbit anti-LAT1 (5347S; Cell Signaling Technology) and mouse anti–β-actin (47778; Santa Cruz Biotechnology, Dallas, Tex) or mouse anti–α-tubulin (T6199; Sigma-Aldrich) as a loading control. Detection of LAT1, LAT2, and CD98 in cell lines (HaCaT, Caco-2, HeLa, and J77) was also conducted in fresh lysates prepared with supplemented RIPA buffer and with the antibodies indicated in Table E1. All primary antibodies were detected with horseradish peroxidase–conjugated goat anti-rabbit (Pierce, Rockford, Ill). Protein bands were analyzed with the LAS-3000 CCD system and Image Gauge 3.4 software (Fuji Photo Film, Tokyo, Japan).

Quantitative profile of L-Leu by using liquid chromatography–tandem mass spectrometry

Serum L-Leu profiles of normal (WT) and immunocompromised *($Rag1^{-/-}$)* mice treated or not with IMQ (for 5 days, 50 mg/d) were measured by using liquid chromatography–tandem mass spectrometry. Serum samples were obtained from at least 20 animals per genotype (10 healthy control mice and 10 mice with psoriasis) after 60 minutes of coagulation at 4°C and were immediately stored at −80°C until use. Stock solutions of leucine (Sigma) and ^{13}C11-Trp (Cambridge Isotope Laboratories, Tewksbury, Mass) were prepared in water (LC/MS grade) at 1000 ppm and used as an external standard and an internal standard, respectively.

Amino acid uptake assays

Naive CD4 T cells obtained from $LAT1^{WT}$, $LAT1^{\Delta R\gamma t}$, and $LAT1^{\Delta CD4}$ mice were cultured (1×10^6 cells/mL) in RPMI medium for 24 hours in the presence of anti-CD3 (5 μg/mL) and used to test amino acid uptake in the presence of LAT1 inhibitors. The ^{3}H-radiolabeled amino acids L-phenylalanine and L-Leu (PerkinElmer, Waltham, Mass) were added (0.5 μCi/ml) in HBSS (Gibco, Carlsbad, Calif) at a final extracellular L-Leu concentration of 5 μmol/L. Amino acid uptake was measured at 60 minutes at 37°C. Incubation with the LAT1 inhibitors JPH203

(10 μmol/L) and 2-aminobicyclo-(2,2,1)-heptane-2-carboxylic acid (40 mmol/L) was done 10 minutes before addition of radioactivity. Uptake was stopped by addition of 20 mmol/L cold L-Leu to quench L-System. At the end of the assay period, cells were harvested onto glass-fiber filters using a Tomtec 96-well parallel harvester (Tomtec, Hamden, Conn). B-radioactivity was counted in a Beckman LS 6500 Multi-Purpose Scintillation Counter (Beckman Coulter, Fullerton, Calif). At least 6 replicates were assessed for each data point.

REFERENCES

E1. Cibrian D, Saiz ML, de la Fuente H, Sanchez-Diaz R, Moreno-Gonzalo O, Jorge I, et al. CD69 controls the uptake of L-tryptophan through LAT1-CD98 and AhR-dependent secretion of IL-22 in psoriasis. Nat Immunol 2016;17:985-96.

E2. Kondo M, Sakuta K, Noguchi A, Ariyoshi N, Sato K, Sato S, et al. Zoledronate facilitates large-scale ex vivo expansion of functional gammadelta T cells from cancer patients for use in adoptive immunotherapy. Cytotherapy 2008;10:842-56.

E3. Taylor PM. Role of amino acid transporters in amino acid sensing. Am J Clin Nutr 2014;99:223S-30S.

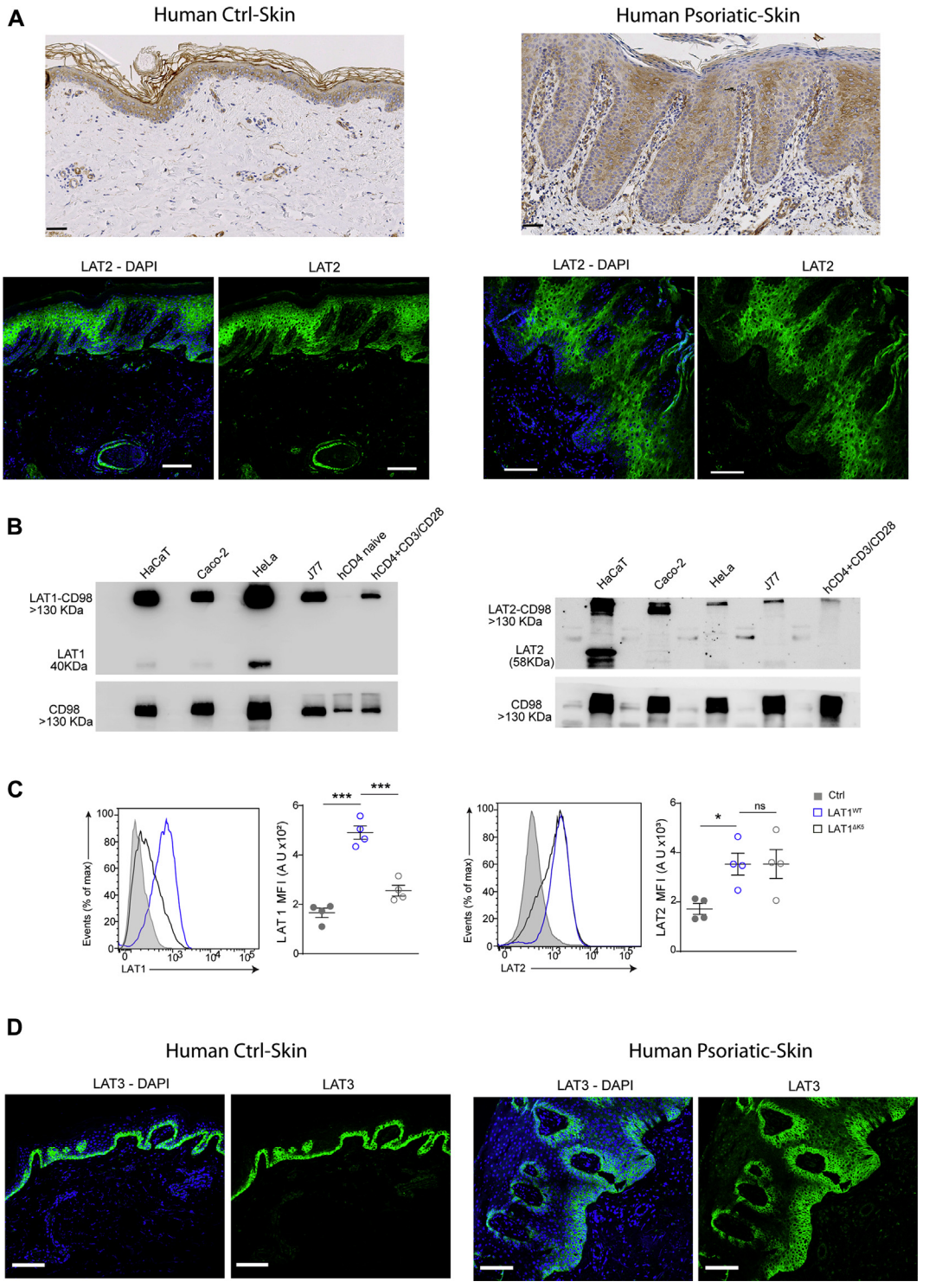

FIG E1. LAT2 and LAT3 expression is detected in the epidermal layer in patients with psoriasis. **A,** LAT2 detection by means of immunohistochemistry *(upper)* and immunofluorescence *(bottom)* in skin biopsy specimens from healthy donors *(left)* and patients with psoriasis *(right)*. **B,** LAT1, LAT2, and CD98 detection by means of Western blotting in nonreduced conditions in 10 μg of total protein from different types of cell lines and primary human CD4 T cells (both naive and activated). **C,** Histograms and values of mean fluorescence intensity of LAT1 *(left)* and LAT2 *(right)* expression in $LAT1^{\Delta K5}$ and $LAT1^{WT}$ keratinocytes after IMQ application. **D,** LAT3 detection by means of immunofluorescence in human skin samples. LAT2 and LAT3 signals are shown in green, and nuclei were stained with 4′-6-diamidino-2-phenylindole dihydrochloride (*DAPI*; blue). *Scale bars* = 100 μm. At least 3 human skin samples of each condition were simultaneously analyzed in each study. A representative experiment of at least 2 individual replicates is shown (n = 4-5; Fig E1, *C*). Data are shown as means ± SEM. *ns*, Not significant. $*P < .05$ and $***P < .001$, 1-way ANOVA with the Bonferroni *post hoc* test.

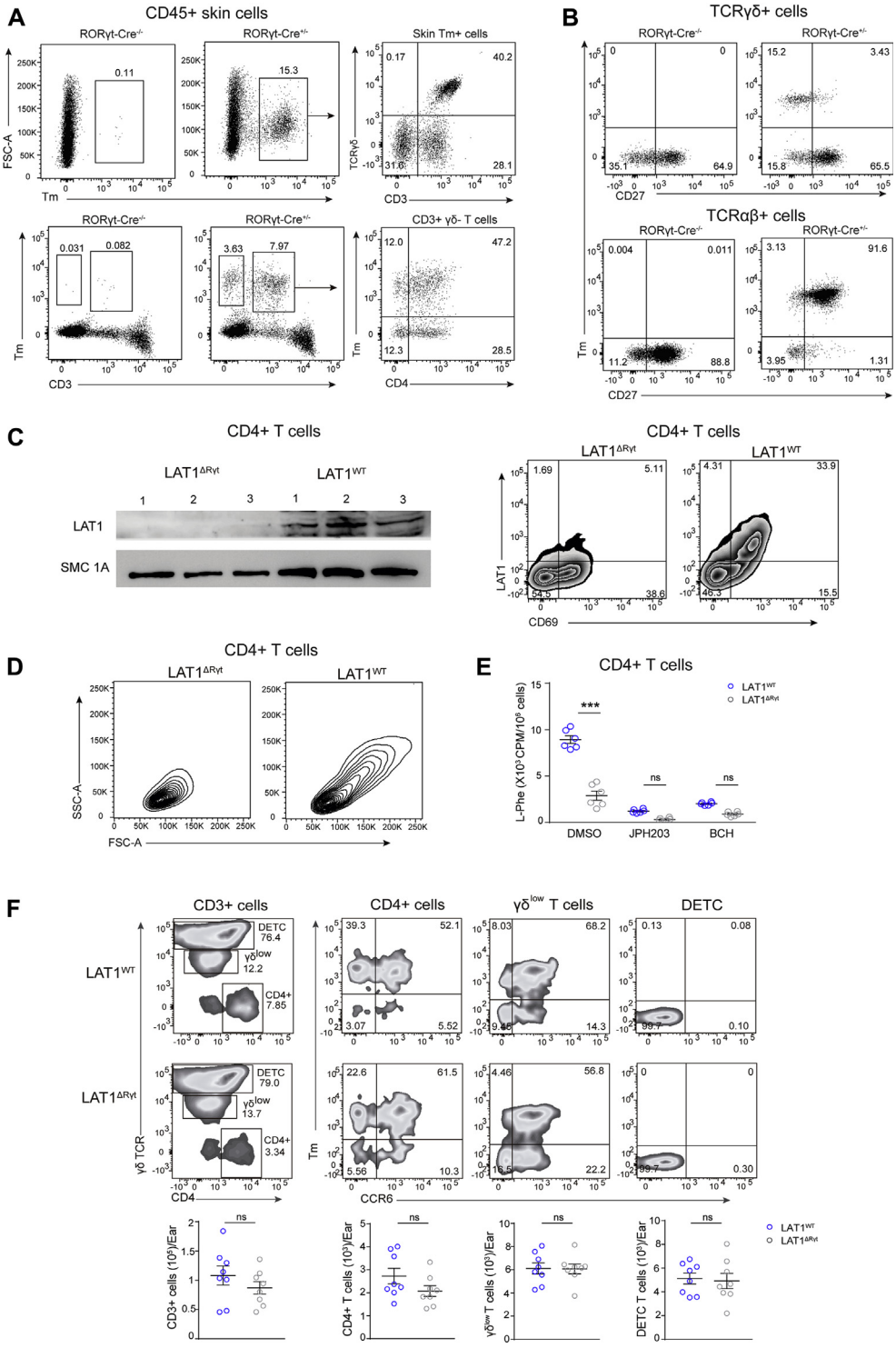

FIG E2. Characterization of immune cells with deletion of LAT1 under the control of RORγt expression. **A,** Skin Tm^+ cells of RORγt-$Cre^{-/-}$ and RORγt-$Cre^{+/-}$ mice were identified as $CD3^{low}$ γδTCR^{low} cells, CD4 T cells, and $CD3^-$RORγt^+ innate lymphoid cells. **B,** Tm expression observed in $CD27^-$ γδ T cells *(upper)* and $CD27^+$ αβ T cells *(bottom)* from RORγt-$Cre^{+/-}$ mice. **C,** LAT1 expression was assessed by using Western blotting *(left)* and FC *(right)* in activated CD4 T cells from $LAT1^{WT}$ and $LAT1^{\Delta Ryt}$ mice. **D,** Size and complexity of cells obtained as in Fig E2, *C*, were evaluated by means of FC. **E,** L-phenylalanine uptake was assessed in activated CD4 T cells from $LAT1^{WT}$ and $LAT1^{\Delta Ryt}$ mice. **F,** Expression of Tm and CCR6 in skin CD4 T cells, dermal γδ T cells ($γδ^{low}$), and epidermal γδ T cells *(DETC)* in $LAT1^{WT}$ and $LAT1^{\Delta Ryt}$ mice are shown. Absolute numbers are shown *(bottom)*. A representative experiment of 2 is shown (n = 3-4 [Fig E2, *A-D*] or n = 6 [Fig E2, *E*]). A pool of 2 independent experiments is shown (n = 4 [Fig E2, *F*]). Data are shown as means ± SEMs. *ns*, Not significant. ***$P < .001$, 2-way ANOVA with the Bonferroni *post hoc* test (Fig E2, *E* and *F*).

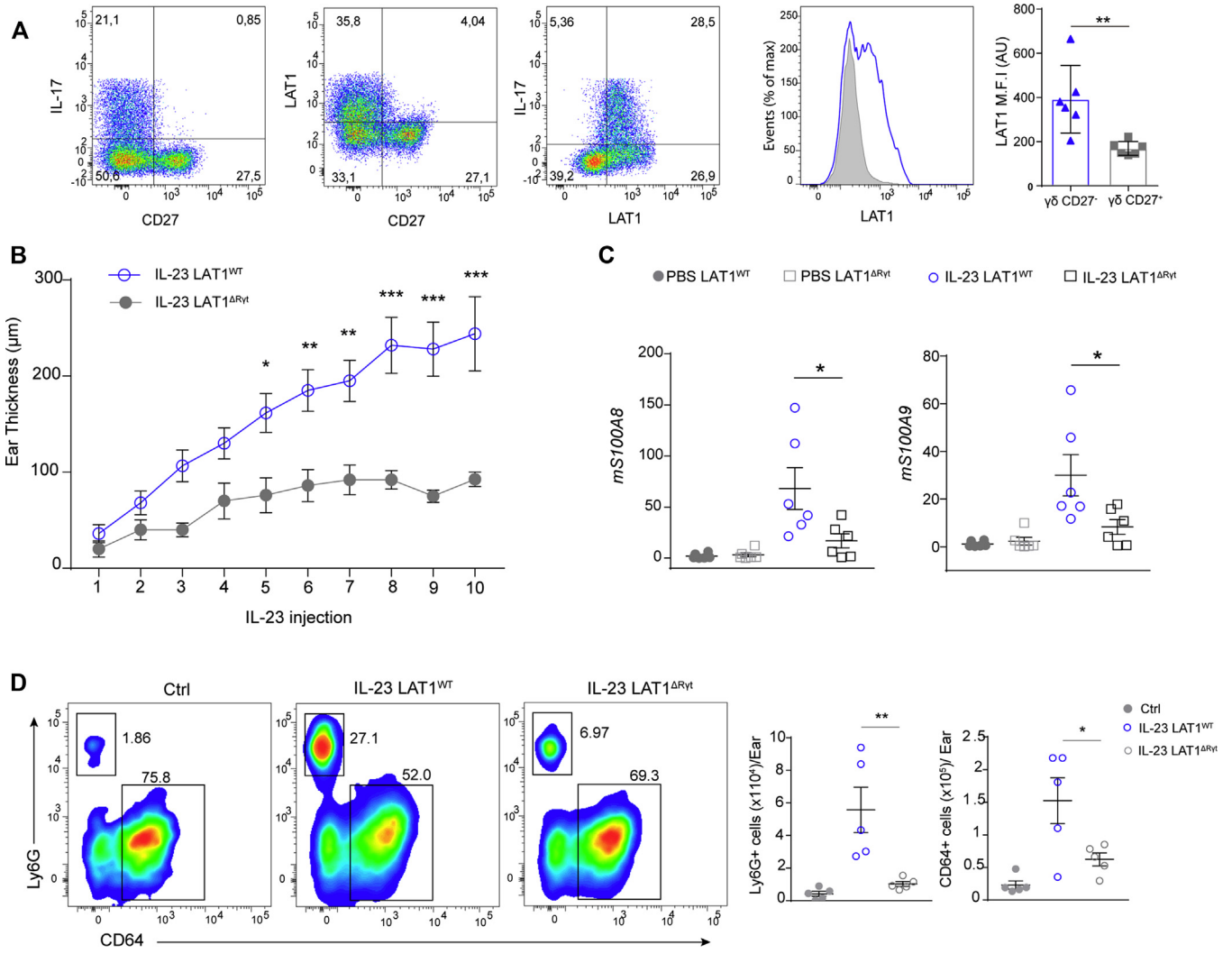

FIG E3. LAT1 expression in IL-17$^+$ γδ T cells controls the IL-23–induced psoriasis model. **A,** Dot plots of lymph node γδ T cells from WT mice after IMQ. Expression of LAT1 in CD27$^-$IL-17$^+$ cells is shown *(dot plots)* and compared with CD27$^+$ γδ T cells (*histograms* and *bars*). **B,** Ear thickness of LAT1$^{\Delta Ryt}$ and LAT1^{WT} mice assessed after IL-23 intradermal injections. **C,** Transcriptional levels of indicated genes in the skin of mice treated with PBS or IL-23. **D,** Representative density plots and density values of neutrophils (Ly6G$^+$) and macrophages (CD64$^+$) infiltrating the skin of mice treated or not with IL-23. A representative experiment of 2 individual replicates is shown (n = 5-6). Data are shown as means ± SEMs. *ns*, Not significant. **P* < .05 and ***P* < .01, 2-tailed unpaired Student *t* test (Fig E3, *A* and *B*) and 1-way ANOVA with the Bonferroni *post hoc* test (Fig E3, *C* and *D*).

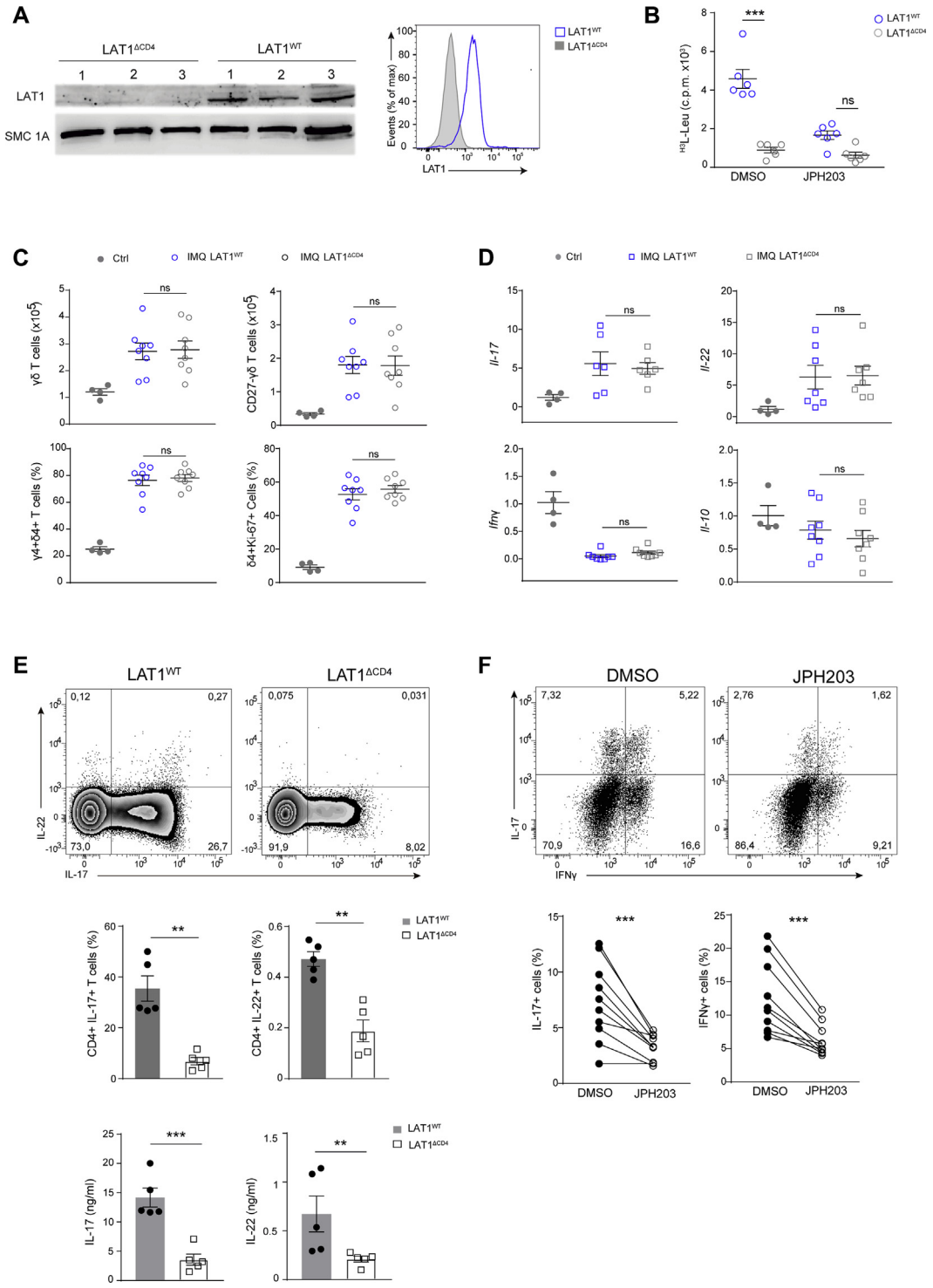

FIG E4. Deletion of LAT1 in CD4 T cells prevents T_H17 differentiation. **A,** LAT1 expression detected by means of Western blotting *(left)* and FC *(right)* in activated CD4 T cells. **B** L-Leu uptake assessed in activated CD4 T cells. **C,** Absolute numbers of γδ *(upper left)* and $CD27^-$ γδ *(upper right)* T cells and frequency of $V\gamma4^+\delta4^+$ T cells *(bottom left)* and $V\delta4^+Ki\text{-}67^+$ cells *(bottom right)* in lymph nodes. **D,** Transcriptional levels of indicated genes in γδ T cells from lymph nodes. **E,** Density plots of mouse T_H17 cells after PMA/ionomycin stimulation *(upper)*. Frequencies of IL-17– and IL-22–secreting cells *(middle)* and cytokine levels (ELISA; *bottom*) are shown. **F,** Human T_H17 cells were obtained in the presence of JPH203 or its vehicle. Representative dot plots after PMA/ionomycin stimulation *(upper)* and frequencies of IL-17– and IFN-γ–secreting cells *(bottom)* are shown. A representative experiment of 2 is shown (n = 3 [Fig E4, *A*]; n = 5-6 [Fig E4, *B* and *E*]; n = 10 [Fig E4, *F*]). A pool of 2 independent experiments is shown (n = 4 [Fig E4, *C* and *D*]). Data are shown as means ± SEMs. *ns*, Not significant. $*P < .05$, $**P < .01$, and $***P < .001$, 2-way ANOVA with the Bonferroni *post hoc* test (Fig E4, *B*), 1-way ANOVA with the Bonferroni *post hoc* test (Fig E4, *C* and *D*), and 2-tailed unpaired (Fig E4, *E*) and paired (Fig E4, *F*) Student *t* tests.

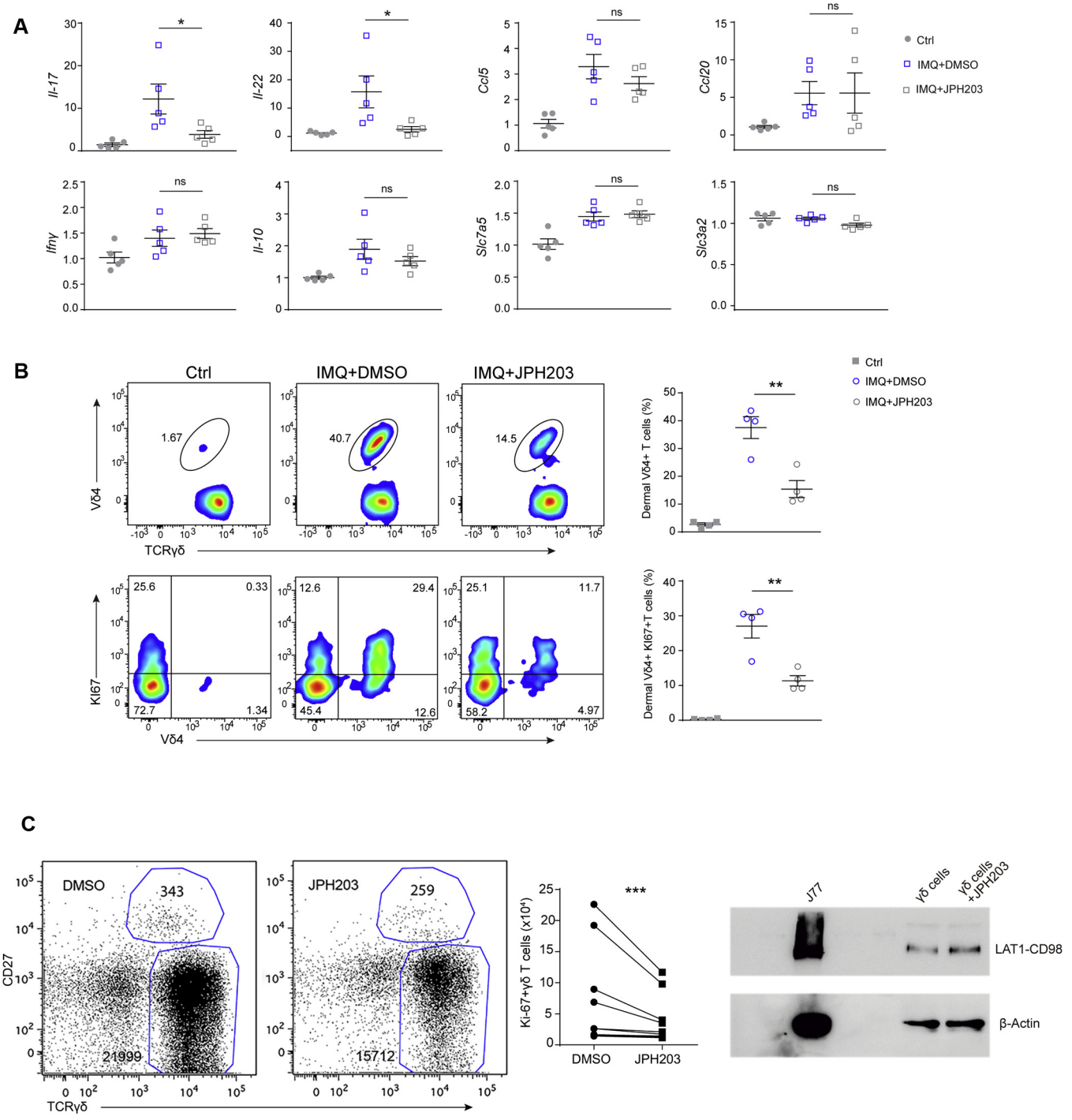

FIG E5. Effects of the LAT1 inhibitor JPH203 in immune cells. **A,** Transcriptional levels of the indicated genes induced in skin-draining lymph node after IMQ. **B,** Density plots *(left)* of the frequency of $V\delta4^+$ *(upper)* and $Ki\text{-}67^+V\delta4^+$ T cells *(bottom)* from the dermal γδ T-cell population. Frequency values are shown at *right*. **C,** Dot plots *(left)* of live human γδ T cells expanded *in vitro* with zoledronate. Values in dot plots indicate total numbers of cells detected in culture after incubation with DMSO or JPH203 normalized by the number of beads. The effect of JPH203 in total γδ T cells obtained from each patient (n = 8 patients) is shown *(middle)*. Representative western blot of purified γδ T cells from one patient to analyze the LAT1-CD98 amino acid complex is shown *(right)*. A representative experiment of 2 is shown (n = 4-5 per group). Data are shown as means ± SEMs. *ns*, Not significant. $*P < .05$, $**P < .01$, and $***P < .001$, 1-way ANOVA with the Bonferroni *post hoc* test (Fig E5, *A* and *B*) and the 2-tailed paired Student *t* test (Fig E5, *C*).

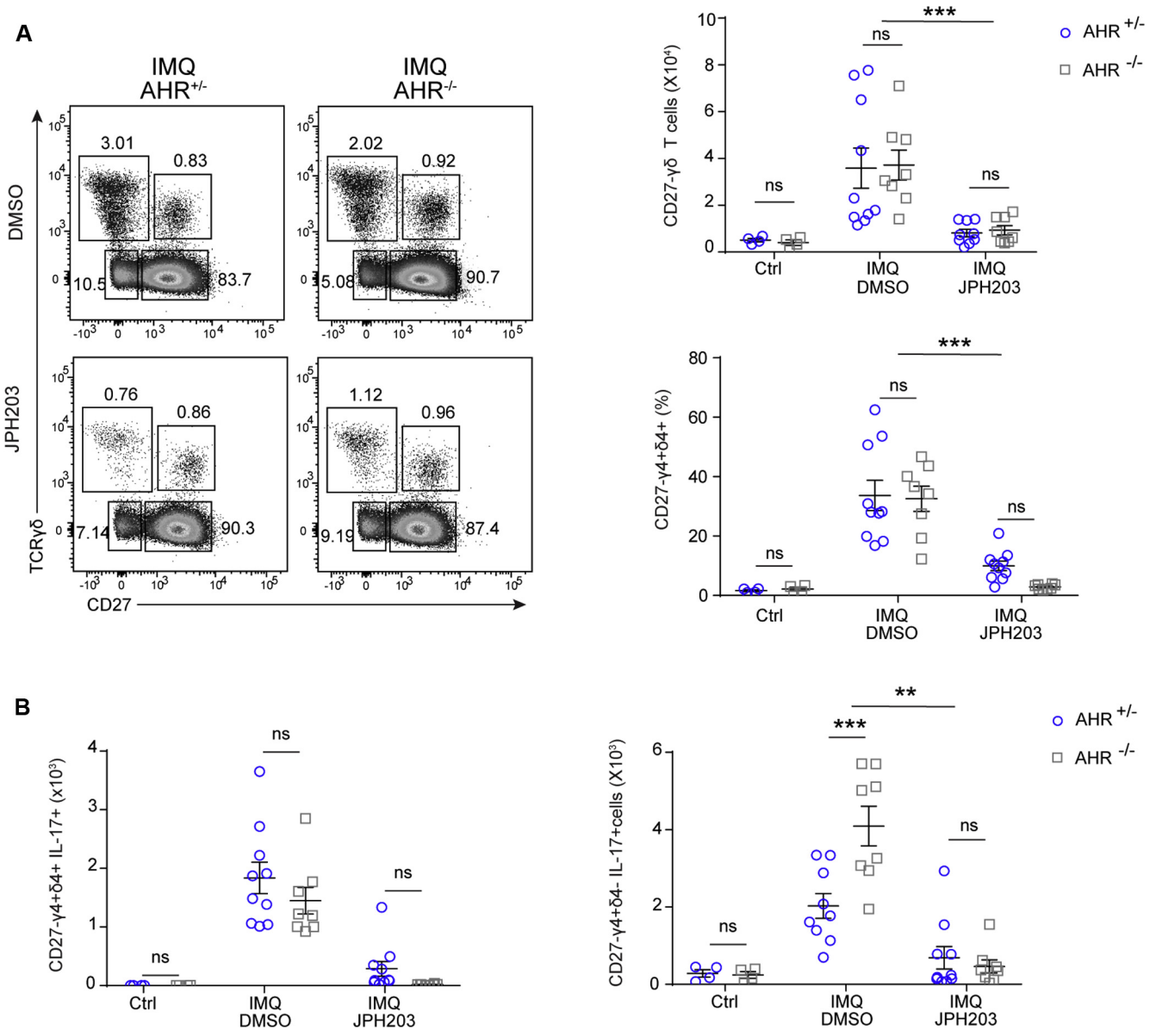

FIG E6. LAT1 inhibition controls γδ T-cell proliferation and IL-17 secretion independently of AHR expression. $AHR^{+/-}$ and $AHR^{-/-}$ mice received IMQ in the ear and were injected with Brefeldin A before death. **A,** Representative dot plots *(left)* and total numbers (*right* and *upper*) of $CD27^{-}$ γδ T cells detected in lymph nodes. Frequencies of $CD27^{-}$ $V\gamma4^{+}\delta4^{+}$ T cells (gated on $CD27^{-}$ γδ T cells) in lymph nodes are also shown (*right* and *bottom*). **B,** Total numbers of $CD27^{-}V\gamma4^{+}\delta4^{+}$ *(left)* and $CD27^{-}V\gamma4^{+}\delta4^{-}$ *(right)* T cells producing IL-17 are shown. Data pools of 2 independent experiments (n = 4) are represented. Data are shown as means ± SEMs. *ns*, Not significant. $^{**}P < .01$ and $^{***}P < .001$, 1-way ANOVA with the Bonferroni *post hoc* test.

TABLE E1. List of used antibodies

Specificity	Reactivity	Clone	Origin	Dilution	Catalog no.
CCR6	Mouse	29-2L17	BioLegend, San Diego, Calif	1:200	129818
CD3e	Mouse	145-2C11	BD Biosciences, San Jose, Calif	1:200	553066
CD4	Mouse	RM4-5	BD Biosciences	1:200	20-0042
CD8	Mouse	53-6.7	BioLegend	1:200	100766
CD11b	Mouse	M1/70	BD Biosciences	1:200	553310
CD11c	Mouse	HL3	BD Biosciences	1:200	557401
CD27	Mouse	LG.7F9	eBioscience, San Diego, Calif	1:200	25-0271-82
CD45.2	Mouse	104	BD Biosciences	1:200	560696
CD64	Mouse	X54-5/7.1	BD Biosciences	1:200	558539
CD98	Mouse	RL388	BioLegend	1:200	128210
CD98	Human, mouse	H300	Santa Cruz Biotechnology, Dallas, Tex	1:500	sc-9160
LAT1	Mouse	H-75	Santa Cruz Biotechnology	1:50	sc-134994
αCD16/αCD32	Mouse	2.4G2	Tonbo Biosciences, San Diego, Calif	1:200	70-0161
IL-17A	Mouse	TC11-18H10	BD Biosciences	1:100	559502
IL-22	Mouse	IL22JOP	eBioscience	1:100	17-7222-82
Ki-67	Mouse	B56	BD Biosciences	1:100	558615
Ly6C	Mouse	AL-21	BD Biosciences	1:200	560525
Ly6G	Mouse	1A8	BD Biosciences	1:200	551461
pS6 (Ser235/236)	Mouse	D57.2.2E	Cell Signaling, Danvers Mass	1:100	8520S
TCRαβ	Mouse	H57-597	BD Biosciences	1:200	109220
TCRγδ	Mouse	GL3	BioLegend	1:200	118118
TCR-Vδ4	Mouse	GL2	BioLegend	1:200	134905
TCR-Vγ4	Mouse	UC3-10A6	BioLegend	1:200	137704
SLC7A5	Human	pAb	Sigma-Aldrich, St Louis, Mo	1:200	HPA052673
SLC7A8	Human, mouse	pAb	Sigma-Aldrich	1:200	HPA051950
SLC43A1	Human	pAb	Sigma-Aldrich	1:200	HPA01882

TABLE E2. Sequences of primers

Gene	Specie	Forward primer	Reverse primer
Actb	Mouse	CAGAAGGAGATTACTGCTCTGGCT	TACTCCTGCTTGCTGATCCACATC
Ccl20	Mouse	ACTGTTGCCTCTCGTACATACA	GAGGAGGTTCACAGCCCTTTT
Ccr6	Mouse	ATGCGGTCAACTTTAACTGTGG	CCCGGAAAGATTTGGTTGCCT
Gapdh	Mouse	AGCTTGTCATCAACGGGAAG	TTTGATGTTAGTGGGGTCTCG
Hprt	Mouse	GCAGTACAGCCCCAAAATGG	GGTCCTTTTCACCAGCAAGCT
Ifng	Mouse	ATGAACGCTACACACTGCATC	CCATCCTTTTGCCAGTTCCT
Il10	Mouse	GCTCTTACTGACTGGCATGAC	CGCAGCTCTAGGAGCATGTG
Il17a	Mouse	TTTAACTCCCTTGGCGCAAAA	CTTTCCCTCCGCATTGACAC
Il22	Mouse	ATGAGTTTTTCCCTTATGGGGAC	GCTGGAAGTTGGACACCTCAA
Il23	Mouse	ATGCTGGATTGCAGAGCAGTA	ACGGGGCACATTATTTTTAGTCT
S100a8	Mouse	AAATCACCATGCCCTCTACAAG	CCCACTTTTATCACCATCGCAA
S100a9	Mouse	ATACTCTAGGAAGGAAGGACACC	TCCATGATGTCATTTATGAGGGC
Slc3a2	Mouse	GACACCGAAGTGGACATGAAA	GCTCCTCCTTGGATAAGCCG
Slc7a5	Mouse	CTGGATCGAGCTGCTCATC	GTTCACAGCTGTGAGGAGC